



Università degli Studi di Ferrara

DOTTORATO DI RICERCA IN  
BIOCHIMICA, BIOLOGIA MOLECOLARE E BIOTECNOLOGIE

CICLO XXV

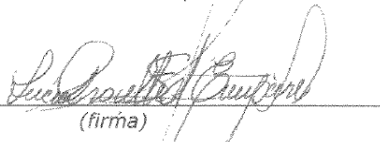
COORDINATORE Prof. FRANCESCO BERNARDI

STRUCTURAL AND FUNCTIONAL STUDIES ON  
*TRYPANOSOMA BRUCEI* 6-PHOSPHOGLUCONATE  
DEHYDROGENASE

Settore Scientifico Disciplinare BIO/10

**Dottorando**

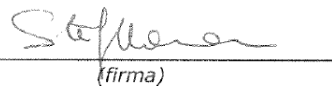
Dott. Proietti-S d'Empaire Lucia Eva



(firma)

**Tutore**

Prof. Hanau Stefania



(firma)

Anni 2010/2012

---

# Contents

	<b>Page</b>
<b>List .of Tables.....</b>	<b>I</b>
<b>List of Figures.....</b>	<b>II</b>
<b>List of Mathematical equations.....</b>	<b>V</b>
<b>I) INTRODUCTION.....</b>	<b>1</b>
1. Human African trypanosomiasis (HAT).....	1
2. Life Cycle of <i>Trypanosoma brucei</i> . Early and Late Symptoms.....	2
3. Epidemiological Studies.....	3
4. Drugs and Target.....	4
5. Structure of 6- phosphogluconate dehydrogenase (6PGDH).....	10
5.a Primary structure.....	10
5.b The 3-dimensional struc.....	11
5.c The <i>T brucei</i> monom.....	12
5.d Coenzyme binding-site.....	13
5.e The dimer interface.....	16
5.f Substrate binding site.....	17
6. Action mechanism of 6-phosphogluconate dehydrogenase.....	19
6.a The two key residues.....	19
6.b Allosteric modulation by the substrate .....	20

6.b.1 Asymmetry .....	20
6.b.2 Other 6PG-induced effects.....	21
6.b.3 Isomerization and allostery.....	22
6.b.4 Other significant effects along the reaction.....	23
<b>II) AIM OF THE THESIS.....</b>	<b>24</b>
1. Structural Studies .....	24
2. Functional Studies.....	24
<b>III) MATERIALS AND METHODS.....</b>	<b>26</b>
1. Site-Directed Mutagenesis .....	26
2. Overexpression of the <i>T. brucei</i> enzyme in <i>E. coli</i> .....	29
3. Purification of 6-PGDH wt / mutant of <i>T. brucei</i> by bacteria <i>E. coli</i> .....	29
4. Determination of protein 6PGDH wt/mutant concentration.....	30
5. Enzyme activity. Assay of activity for 6PGDH.....	31
6. Cysteines reactivity.....	31
7. Polyacrylamide gel electrophoresis (SDS PAGE).....	31
8. Gel Filtration (SEPHACRYL S 200 and AcA 34).....	34
9. Chemical cross-linking of 6PGDH.....	35
10. Dynamic Light scattering (DLS) measurements.....	38
11. Sucrose-density-gradient centrifugation.....	41
12. Isothermal titration calorimetry (ITC) studies.....	42
12.a Preparation of the sample and the ligand.....	44
12. a.1 enzyme preparation.....	44
12.a.2 ligand preparation.....	45
12.b Setting up the Experiment.....	45

12.c Data processing using software provided by the OriginTM.....	46
12.c.1 Changes in heat capacity ( $\Delta C_p^\circ$ ).....	48
12.c.2 Effect of pH on dissociation constant .....	49
12.c.3 ) Effect of pH on binding enthalpy.....	49

## IV) RESULTS, ANALYSIS AND CONCLUSIONS

### Part I. Structural studies.

• <i>Results and Discussion</i> .....	<b>52</b>
a) Gel-filtration of 6PGDH.....	52
b) Velocity Sedimentation of 6PGDH.....	53
c) Glutaraldehyde cross-linking of 6PGDH.....	54
d) Dynamic light scattering.....	57
e) Calculation of heat capacity change ( $\Delta C_p$ ) by microcalorimetry.....	57
f) Dimer-tetramer equilibrium in 6PGDH mutants.....	60
• <i>Conclusion</i> .....	<b>61</b>

### Part II. Functional studies.

• <i>Results and Discussio</i> .....	<b>63</b>
<b>a) Effect of mutation on the enzyme activity</b> .....	<b>64</b>
a.1) E192Q.....	64
a.2) K185H.....	64
a.3) H188L .....	65
<b>b) Cysteine reactivity</b> .....	<b>65</b>
<b>c) 6PG binding to 6PGDH</b> .....	<b>67</b>
c.1) The binding of 6PG to 6PGDH WT.....	67

c.2) The binding of 6PG to E192Q mutant.....	69
c.3) The binding of 6PG to K185H mutant.....	70
c.4) The binding of 6PG to H188L mutant.....	70
• <i>Conclusion</i> .....	75
<b>V) REFERENCES</b> .....	<b>76</b>
<b>VI) DECLARATION OF CONFORMITY</b> .....	<b>84</b>

---

# List of Tables

	Pag
<i>INTRODUCTION</i>	
<b>Table 1:</b> HAT drugs in clinical use.....	5
<b>Table 2:</b> 6PGDH inhibition constants of compounds.....	10
<i>MATERIALS AND METHODS</i>	
<b>Table 3.</b> Primer oligonucleotides synthesized .....	27
<b>Table 4:</b> The protocol Mutagenesis reaction.....	27
<b>Table 5:</b> The temperature cycling. Mutagenesis reaction.....	27
<b>Table 6:</b> the stacking gel solution 5% (w/v). SDS PAGE.....	33
<b>Table 7:</b> Coomassie blue C250 without methanol for SDS-PAGE.....	34
<b>Table 8:</b> pK and $\Delta H$ ionization of buffers used for Isothermal titration calorimetry (ITC) studies.....	46
<i>RESULTS ANALYSIS AND CONCLUSIONS I</i>	
<b>Table 9:</b> DLS measurements of mean hydrodynamic radius. ....	57
<b>Table 10:</b> Comparison between the changes in the subunit polar and apolar solvent exposed surface area ( $\Delta ASA_p$ and $\Delta ASA_{ap}$ in $\text{\AA}^2$ ).....	59
<b>Table 11:</b> Binding parameters of NADP to 6PGDH from <i>Trypanosoma brucei</i> .....	61
<i>RESULTS ANALYSIS AND CONCLUSIONS II</i>	
<b>Table 12.</b> Intrinsic $K_d$ , $pK_a$ and number of proton exchanged at the 6PG binding.....	67
<b>Table 13.</b> Buffer-independent enthalpy change and number of hydrogen ions exchanged at different pH in the mutant E192Q at the 6PG binding.....	69

---

# List of Figure

	Pag
<i>INTRODUCCTION</i>	
<b>Figure 1:</b> WHO Report on Global Surveillance of Epidemic –prone Infectious Diseases - African trypanosomiasis .....	4
<b>Figure 2:</b> Pentose Phosphate Pathway.....	7
..	
<b>Figure 3:</b> Reaction catalyzed by 6-PGDH and the two main amino acid residues involved .....	8
<b>Figure 4:</b> Structures of some substrate analogues of 6PGDH.....	9
<b>Figure 5:</b> Multiple alignment of 6PGDH from several species .....	12
<b>Figure 6:</b> Monomer of the <i>T. brucei</i> 6PGDH .....	13
<b>Figure 7:</b> Coenzyme binding site of the <i>T. brucei</i> 6PGDH .....	14
<b>Figure 8:</b> Dimer of the <i>T. brucei</i> 6PGDH .....	16
<b>Figure 9:</b> Substrate binding site of the <i>T. brucei</i> 6PGDH .....	17
<b>Figure 10:</b> <i>T. brucei</i> 6PGDH active site with the position of the two residues, discussed in the introduction .....	19
<b>Figure 11:</b> Half of the site mechanism. ....	20
<b>Figure 12:</b> Alternating site co-operativity model for the enzyme 6PGDH .....	22

## MATERIALS AND METHODS

<b>Figure 13:</b> Scheme of the QuickChange II site-directed mutagenesis method .....	26
<b>Figure 14:</b> Reaction of the amino groups of proteins with glutaraldehyde.....	36
<b>Figure 15:</b> Formation of pyridine rings after the reaction of glutaraldehyde with amino groups of proteins.....	37
<b>Figure 16:</b> Summary of the possible forms of glutaraldehyde in aqueous solution.....	37
<b>Figure 17 :</b> Collecting of the fractions after the density-gradient centrifugation.....	42
<b>Figures 18 :</b> Schematic representation of a VP-ITC microcalorimeter and the syringe.....	43

## RESULTS ANALYSIS AND CONCLUSIONS I

<b>Figure 19:</b> Gel-filtration profile of <i>T. brucei</i> 6PGDH with and without either NADPH or other ligands.....	52
<b>Figure 20.</b> Sedimentation of <i>T. brucei</i> 6PGDH with and without 0.02 mM NADPH or with both NADPH and 0.16 mM 6PG .....	53
<b>Figure 21.</b> Enzyme concentration dependence of the association reaction between dimers to form tetramer for <i>T. brucei</i> 6PGDH, in absence or presence of 0.02 mM NADPH.....	54
<b>Figure 22.</b> SDS-PAGE at 7,5 % acrylamide in the resolving gel, of chemically cross-linked <i>T. brucei</i> 6PGDH, in the absence (A) and presence (B) of 40 $\mu$ M NADPH, with glutaraldehyde.....	55
<b>Figure 23.</b> SDS-PAGE of <i>T. brucei</i> 6PGDH, treated for different times with glutaraldehyde .....	56



<b>Figure: 24.</b> <i>T. brucei</i> 6PGDH titration with NADP by ITC, in Hepes buffer, pH 7.5 .....	58
<b>Figure 25.</b> Buffer-independent enthalpy change ( $\Delta H_0$ ) dependence from the temperature for the binding to <i>T. brucei</i> 6PGDH of NADP and NADPH.....	59
 <i>RESULTS ANALYSIS AND CONCLUSIONS II</i> 	
<b>Figure 26.</b> pK <sub>m</sub> dependence from pH for 6PG in <i>T. brucei</i> 6PGDH .....	63
<b>Figure 27.</b> Kinetics of the mutant K185H.....	65
<b>Figure 28.</b> The cysteines reactivity in absence and in presence of 6PG for WT and H188L mutant.....	66
<b>Figure 29.</b> pH dependence for 6PG apparent pK <sub>d</sub> .....	68
<b>Figure 30.</b> Scheme with three residues involved in the change of the protonation state of the enzyme at the substrate binding.....	68
<b>Figure 31:</b> Kinetic mechanism of 6PGDH.....	71
<b>Figure 32:</b> Scheme for the pK <sub>a</sub> shifts for ionizable residues in the <i>T. brucei</i> 6PGDH.....	74

---

# List of Mathematical Equations

MATERIALS AND METHODS	Pag
<i>Dynamic Light Scatering Data processing</i>	
<b>Equation 1:</b> The wave vector.....	38
<b>Equation 2:</b> Correlation function. of the scattering signal.....	39
<b>Equation 3:</b> equation for single exponential decay for the correlation function.....	39
<b>Equation 4:</b> The Stokes-Einstein relation.....	40
<i>ITC Data processing</i>	
<b>Equation 5:</b> the Gibbs free energy.....	46
<b>Equation 6:</b> the Gibbs free energy .....	47
<b>Equation 7:</b> Observed enthalpy equation ( $\Delta H_{obs}$ ).....	47
<b>Equation 8:</b> Number of hydrogen ions released or taken.....	47
<i>ITC Data processing. Changes in heat capacity (<math>\Delta C_p^\circ</math>)</i>	
<b>Equation 9:</b> Changes in heat capacity ( $\Delta C_p$ ) from exposed surfaces variations.....	48
<b>Equation 10:</b> $\Delta H$ reference value obtained at the temperature (60 °C).....	48
<i>ITC Data processing . Effect of pH on dissociation constant</i>	
<b>Equation 11:</b> The intrinsic dissociation constant ( $K_{app}$ ) .....	49
<i>ITC Data processing Effect of pH on binding enthalpy</i>	
<b>Equation 12:</b> The capture/release of hydrogen ions ( $nH^+$ ) depending on the pH and pKa.....	49
<b>Equation 13:</b> enthalpy changes as a function of the protonation / deprotonation and the intrinsic enthalpy binding .....	50

<b>Equation 14:</b> $\Delta H_o$ transformed.....	50
<b>Equation 15:</b> V/K equation.....	71

---

# INTRODUCTION

## 1) Human African trypanosomiasis

The Kinetoplastida are a protozoan class belonging to the Excavata supergroup, encompassing numerous medically and agriculturally important pathogens, as well as free-living representatives that have huge ecological impact.[4].

Within the kinetoplastida, the order Trypanosomatida contains many pathogens, including *Trypanosoma brucei*, *T. cruzi* and *Leishmania* spp., the causative agents of African trypanosomiasis, Chagas' disease and leishmaniasis respectively. These parasites have evolved diverse immune evasion strategies; while *Leishmania* spp. and *T. cruzi* exploit intracellular lifestyles by invasion of host cells, *T. brucei* persists within the host bloodstream and lymphatic system, and is therefore continually exposed to both innate and adaptive immune mechanisms. The surface of mammalian infective *T. brucei* is dominated by approximately  $2 \times 10^7$  molecules of a single GPI-anchored variant surface glycoprotein (VSG), shielding invariant surface antigens from antibody recognition[4].

*Trypanosoma brucei brucei* causes the veterinary disease Nagana, but it is unable to establish infections in humans. Human resistance to *T. brucei brucei* infection is due to the presence of a trypanolytic component of human serum, which provides innate immunity against infection. This component is a minor subfraction of high-density lipoproteins (HDLs) called the trypanosome lytic factor 1 (TLF-1). This toxic class of HDLs is internalized in *T. brucei brucei* via receptor-mediated endocytosis and is ultimately targeted to the lysosome, where it initiates low-pH-dependent killing. However, *T. b. rhodesiense* and *T. b. gambiense*, managed to escape this immunity system, enabling them to grow in humans where they cause sleeping sickness, as Human African Trypanosomiasis (HAT) is called.[5]

The mechanism of resistance to TLF-1 remains to be fully elucidated; however, it is well established that the resistance phenotype of *T. brucei gambiense* (chronic form of the disease in West Africa- Congo) and *T. brucei rhodesiense* (acute form in Est Africa- Zimbabwe, Tanzania, Zambia, Angola (Figure 1) is due to the expression of the serum resistance associated (SRA) protein (a member of the VSG gene family). [1].

## **2) Life Cycle of *Trypanosoma brucei*. Early and Late Symptoms**

Both trypanosomes are morphologically identical and are transmitted to human hosts by bites of infected tsetse flies (*Glossina palpalis* transmits *T. brucei gambiense* and *Glossina morsitans* transmits *T. brucei rhodesiense*), which are found only in Africa. [2].

Life cycle of the parasites starts when the trypanosomes are ingested during a blood meal by the tsetse fly from a human reservoir in West African trypanosomiasis or an animal reservoir in the East African form. The trypanosomes multiply over a period of 2-3 weeks in the fly midgut; then, the trypanosomes migrate to the salivary gland, where they develop into epimastigotes. The metacyclic trypomastigotes infect humans, following a fly bite, which occasionally causes a skin canker at the site [54].

In the first stage, the trypanosomes multiply in subcutaneous tissues, blood and lymph. This is known as a haemolymphatic phase, which entails bouts of fever, headaches, joint pains and itching.

In the second stage the parasites cross the blood-brain barrier to infect the central nervous system. This is known as the neurological phase. In general this is when more obvious signs and symptoms of the disease appear: changes of behaviour, confusion, sensory disturbances and poor coordination. Disturbance of the sleep cycle, which gives the disease its name, is an important feature of the second stage of the disease. Without treatment, sleeping sickness is considered fatal. The first stage of *T. brucei gambiense* sleeping sickness is long and relatively asymptomatic [55].

### **3) Epidemiological studies**

Epidemiological studies indicate that this disease threatens millions of people in 36 countries in sub-Saharan Africa. Many of the affected populations live in remote areas with limited access to adequate health services, which hampers the surveillance and therefore the diagnosis and treatment of cases. In addition, displacement of populations, war and poverty are important factors leading to increased transmission and this alters the distribution of the disease due to weakened or non-existent health systems. [8]

In 2009, after continued control efforts, the number of cases reported has dropped below 10 000 for the first time in 50 years. This trend has been maintained in 2010 with 7139 new cases reported (WHO). Despite these efforts, the problematic of internal conflicts by armed groups has impaired the work of sanitary control of active outbreaks of disease as well as promoted the mobilization of citizens to areas where they are more exposed to the vector and access to health centre to treat the disease is less or naught.

Additionally cases of African trypanosomiasis have been reported in recent years in travellers coming from various parts of Africa, particularly from the natural parks of Tanzania [6;7]

This means that although African trypanosomiasis is endemic in an area of Africa, there is a high risk factor for travellers.

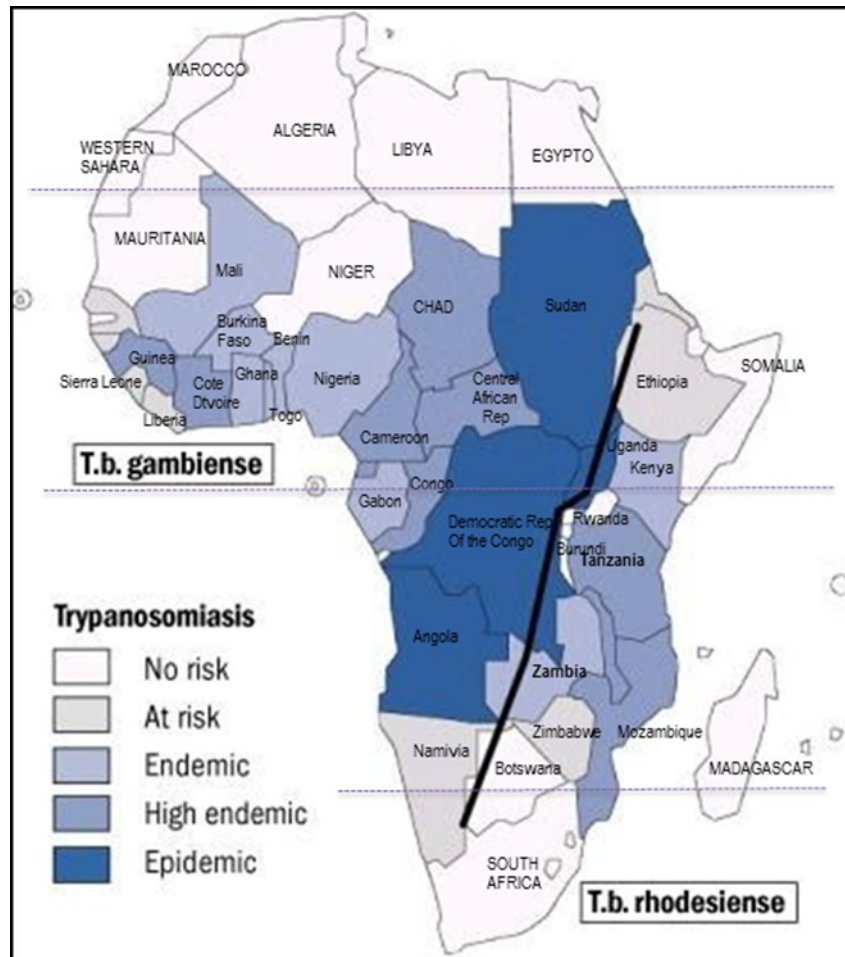


**Figure 1:** WHO Report on Global Surveillance of Epidemic -prone Infectious Diseases African trypanosomiasis

#### 4) Drugs and target

Currently development of effective vaccines against these parasites remains an unrealized goal and clinical management is based on chemotherapeutics. Cost, toxicity and resistance problems of conventional drugs result in an urgent need to identify and develop new therapeutic alternatives. Traditionally, neglected tropical diseases have not been the focus of robust efforts to identify new drugs due to lack of a profitable market and effective strategies to implement control programmes [9].

The global effort to control the infection is based on a combination strategy of vector control and drug treatment of infected patients. Currently there is no drug that is effective against both stages of the disease or both subspecies, and all therapies require parenteral

administration (Table 1). Early-stage disease is treated with pentamidine (*T. b. gambiense*) or suramin (*T. b. rhodesiense*) [9], but both compounds show some toxicity.

Suramin has been reported to inhibit a number of glycolytic enzymes [10], including a recent report that it inhibits pyruvate kinase by binding the ATP site as shown by X-ray structure analysis [11].

Treatment of late-stage disease is more problematic. Historically the highly toxic arsenical compound melarsoprol was used to treat both subspecies of the disease, causing 5–10% fatality in treated patients. However in 2009 a new nifurtimox/eflornithine combination therapy (NECT) was advanced for the treatment of late-stage *T. b. gambiense* after showing equivalent to better efficacy than eflornithine (DFMO) alone in clinical trials. NECT has not yet been tested against *T. b. rhodesiense*, and despite improvements over eflornithine alone, administration still requires 7 days of twice daily i.v. infusions of eflornithine along with oral nifurtimox administration. [9].

Compound	Indication/limitations/status	Dosing method	Mechanism of action
Suramin	Used for the treatment of early-stage <i>T. b. rhodesiense</i> ; does not cross the blood brain barrier	IV injection	Unknown; binds to pyruvate kinase (Morgan <i>et al.</i> , 2011) contribution to toxicity unknown; lysosomal proteins contribute to activity (Alsford <i>et al.</i> , 2012)
Pentamidine	Used for the treatment of early-stage <i>T. b. gambiense</i> ; does not cross the blood brain barrier	IM injection	Unknown; analogues collapse the mitochondrial membrane potential but protein target unknown (Lanteri <i>et al.</i> , 2008); P-type ATPases contribute to uptake (Alsford <i>et al.</i> , 2012)
Melarsoprol	Late stage, all strains; currently recommended only for late-stage <i>T. b. rhodesiense</i> ; highly toxic	IV infusion	Unknown; forms a stable adduct with trypanothione, role in toxicity unknown
Eflornithine	Late stage, <i>T. b. gambiense</i> recommended therapy in combination with nifurtimox	IV infusions	Inhibitor of ornithine decarboxylase (Jacobs <i>et al.</i> , 2011a)
Nifurtimox	Late stage, <i>T. b. gambiense</i> in combination with eflornithine	Oral	Activation by a type I nitroreductase required (Wilkinson <i>et al.</i> , 2008; Hall <i>et al.</i> , 2011)
SCYX-7158	Phase I started. Target profile, both stages and strains	Oral	Unknown
Fexinidazole	Phase I complete; Phase II/III scheduled. Target profile, both stages and strains	Oral	Unknown, but activation by a type I nitroreductase is required in leishmania (Wyllie <i>et al.</i> , 2012)

**Table 1:** HAT drugs in clinical use.

The organization Drugs for Neglected Diseases Initiative (DNDi) is emphasizing development of new compounds, such as oxaborole SCYX-7158 and fexinidazole for the treatment of both early and late-stage disease and they are currently undergoing clinical trials [9].

Eflornithine target has been shown to be ornithine decarboxylase, an essential enzyme in the biosynthesis of polyamines [12]. Regarding nifurtimox, there is good evidence that activation by a type I nitroreductase leading to production of intracellular free radicals, is



key to its efficacy [13;16]. Analogues of pentamidine have been shown to collapse the mitochondrial membrane potential but the protein targets that mediate these effects are unknown [14]. Recent efforts to utilize genome-wide RNAi approaches have led to the identification of genes involved in suramin uptake, and to the identification of several other lysosomal proteins that contribute to its action [15]. However, for pentamidine, suramin and melarsoprol, a number of genes were identified that modulate their function, suggesting that clear identification of their molecular targets will not be straightforward [9].

Others proteins such as trypanothione reductase, which are unique for trypanosomes, have been proposed as ideal target [9]. However also other enzymes, which are present both in parasites and in the guests, may be effective targets, if they have structural characteristics that may be subject to selective inhibitors, such the case of ornithine decarboxylase. This was clearly demonstrated also in the case of the enzyme of glycolysis glyceraldehyde-3-phosphate dehydrogenase (GAPDH). Differences in the binding site of the coenzyme (NAD<sup>+</sup>) were identified using a comparative analysis by X-ray crystallography [10]. Structures adenosine-based, as analogues of the co-factor, have been shown to selectively inhibit the enzymes of trypanosome and also to kill both *T. brucei* and *T. cruzi*. [19].

The bloodstream-form of *T. brucei* has the blood glucose as the sole source of nutrition. For this reason, the glycolysis that is responsible for substrate-level ATP production in the cell, was considered a good target for the development of new drugs. The absence of glucose or incubation of the parasite with inhibitors of certain glycolytic enzymes, leads to a rapid lysis and death of the parasite present in the bloodstream of the host. Also demonstrations based on mathematical models and experiments of gene knock-out revealed that glycolysis is essential and validated this pathway as drug target. [18, 52]

Glycosomes are a specialized form of peroxisomes (microbodies) present in unicellular eukaryotes that belong to the Kinetoplastea order, such as Trypanosoma and Leishmania species. The organelles harbour most enzymes of the glycolytic pathway [52]. Some drug targets may be found in the glycosomes compartments, and in the metabolism of lipids and of purines too [6].

The pentose phosphate pathway also plays a crucial role in the metabolism of the parasite and in the host-parasite relationship, since its main function is the production of NADPH, which is necessary for the defense against oxidative stress and for different reductive biosynthetic reactions. (Figure 2).

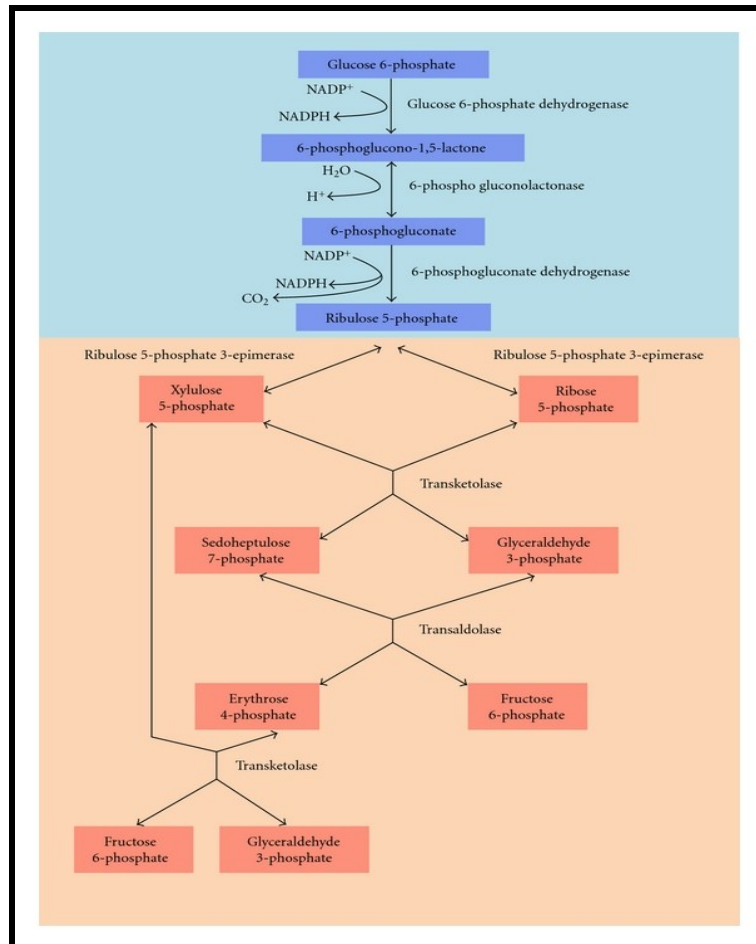


**Figure 2:** Pentose Phosphate Pathway. 6PGDH is the third enzyme of the Pentose Phosphate Pathway (Gupta S et al 2011)

The decrease of the availability of this reduced coenzyme increases susceptibility to oxidative stress and hampers the reductive biosyntheses of the parasite. [20].

6-phosphogluconate dehydrogenase (6PGDH) is the third enzyme of the pentose phosphate pathway, it catalyzes the oxidative decarboxylation of 6-phosphogluconate (6PG) to ribulose-5-phosphate (RU5P), with redox reaction preceding decarboxylation, via 3-keto 6PG and a probable 1, 2-enediol as intermediates (Figure 3)

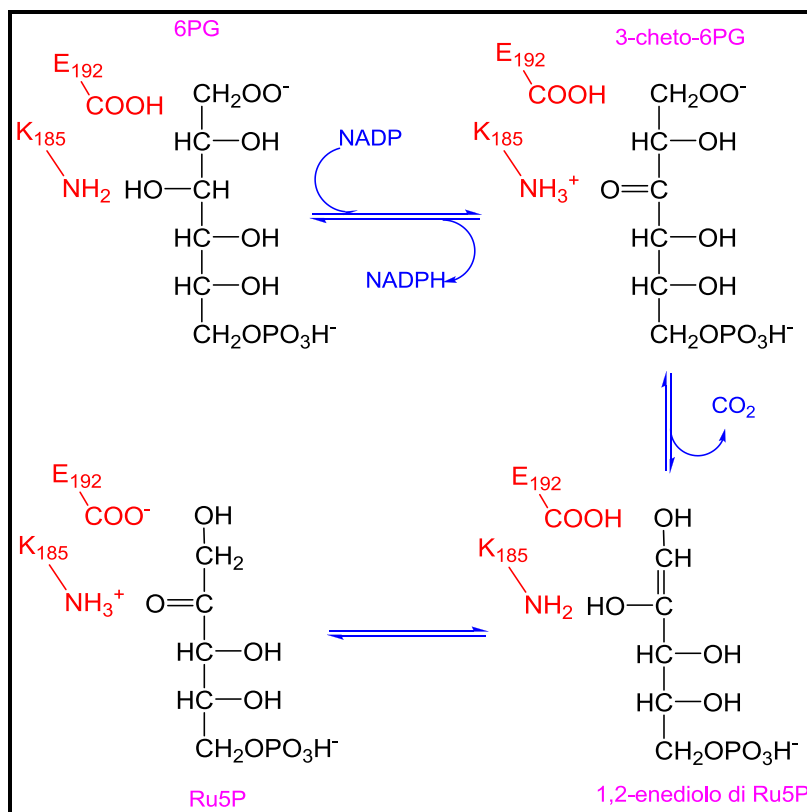


**Figure 3:** reaction catalyzed by 6-PGDH and the two main amino acid residues involved

The inhibition of 6PGDH causes an accumulation of 6PG in the cell, which acts as an inhibitor of 6-phosphogluconate isomerase, the enzyme that converts glucose-6-phosphate to fructose-6-phosphate during glycolysis. The accumulation of glucose-6-phosphate in the cell addresses this to enter the pentose phosphate pathway by triggering a positive feedback loop that feeds on itself with fatal consequences for the parasite. [21].

Enzyme inhibition studies have shown that there are strong inhibitors against 6PGDH, which show some selectivity versus the parasite enzyme compared the mammalian one. *T. brucei* 6PGDH shows only a 33% amino acid identity with the mammalian 6PGDH even if their structures have a similar overall fold and many residues nearest neighbours to the substrate are conserved [22]

Three reviews have dealt with *T. brucei* 6PGDH inhibitors as lead compounds for new drugs against African trypanosomes [21,23,53]. Inhibitors have been found, which mimic the transition-state and high-energy intermediates of the enzymatic reaction of 6PGDH [24]. Hydrophobic analogues of these also revealed some anti-parasite activity [25]. A

number of phosphorylated carboxylic acids derived from aldose sugars were tested against 6PGDH, two particularly notable inhibitors were identified. Both 4-phospho-D-erytronate (4PE) and 5-phospho-D-ribonate (5PR) (Fig. 4, compounds **1** and **2**) were competitive with respect to substrate, with  $K_i$  values for the *T. brucei* 6PGDH equal to 130 and 950 nM, respectively.

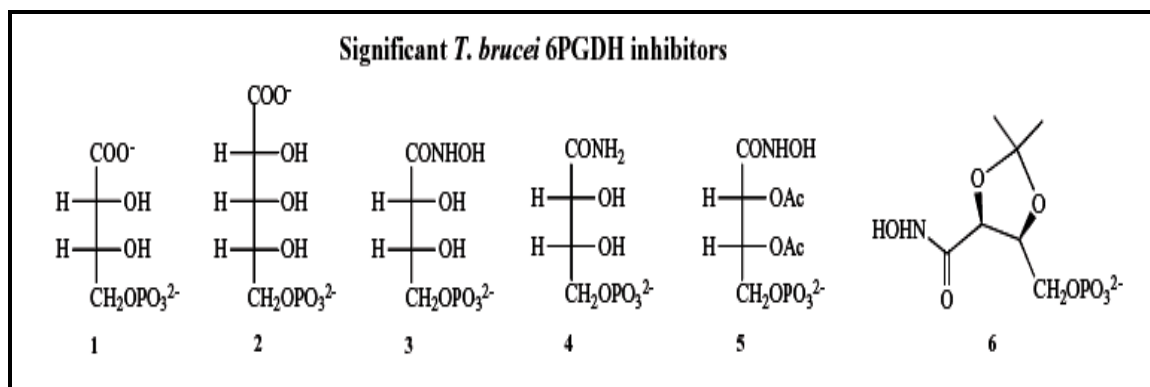


**Figure 4:** Structures of some substrate analogues (Ac=Acetyl group). . 4-phospho-D-erytronate (compounds **1**); 5-phospho-D-ribonate (compounds **2**) ; 4-phospho-D-erythronohydroxamate (compound **3**), 4-phospho-D-erythronamide (compound **4**) and two protected analogues of 4-phospho-D-erythronohydroxamate (compounds **5** and **6**)

Their selectivities for the *T. brucei* 6PGDH over the sheep liver one (ratio  $K_i$  sheep/  $K_i$  *T. brucei*) were measured at 83-fold and 70-fold respectively.  $K_i$  values for both are under the  $K_m$  for 6PG (= 3.5  $\mu$ M), indicating that they mimic high energy reaction intermediates ( Figure 3) rather than the substrate *per se* [21,26, 19].

Another potent and selective *T. brucei* 6PGDH inhibitor is 4-phospho-D-erythronohydroxamate (Figure 4, compound **3**), synthesized specifically to mimic the high-energy intermediates produced following the second (decarboxylation) step of the catalyzed reaction, shown in Figure 3 . This hydroxamate, with a  $K_i$  = 10 nM and selectivity of 254-fold for the parasite enzyme over the sheep liver enzyme, is the compound with the highest affinity for the *T. brucei* 6PGDH reported to date and it also shows the highest selectivity for the parasite over the sheep liver enzyme [24]. In Table 2, inhibition constants versus 6PG ( $K_i$ ) at pH 7.5 (which is the enzyme optimum pH) for all *T. brucei* 6PGDH inhibitors, which are shown in the figures included in this text, are

reported, together with selectivity values over the sheep liver enzyme (ratio sheep liver 6PGDH  $K_i$  / *T. brucei* 6PGDH  $K_i$ ).

Compound	$K_i$ versus substrate ( $\mu$ M)	Selectivity ( $K_i$ sheep/ $K_i$ <i>T. brucei</i> )
1	0.13	83
2	0.95	70
3	0.01	254
4	1.52	25.7
5	0.08	4.5
6	0.035	31.4

**Table 2:** 6PGDH inhibition constants of compounds in figure 4.. 4-phospho-D-erythronate (compounds **1**); 5-phospho-D- (compounds **2**) ; 4-phospho-D-erythronhydroxamate(compound **3**) ; 4-phospho-D-erythronamide (compound **4**) and two protected analogues of 4-phospho-D-erythronhydroxamate (compounds **5** and **6**)

Genetic studies and RNA interference, which leads to the selective suppression of the expression of a gene, are today highly used, also for their extreme speed, to verify the effect of inhibition of an enzyme in the parasite [21]. These studies have indicated that in *T. brucei* 6PGDH can be a drug target since expression of the gene encoding 6PGDH has been shown essential for growth of *T. brucei* bloodstream form.

## 5) Structure of 6-phosphogluconate dehydrogenase

### 5.a) Primary structure

The comparative study of the amino acid sequence, using alignment, has revealed a 33% identity between the amino acid sequence of *T. brucei* 6PGDH and mammalian enzyme

[43] while identity is somewhat higher (37.3%) both with the chloroplast and the cytosolic 6PGDH from spinach [42].

This may reflect the evolutionary history of the kinetoplastids, the phylogenetic order to which trypanosomes belong, which have been proposed to have derived from an ancestor common with the primitive plants Euglenoid algae [40].

Furthermore the closer relationship between the genes of *Trypanosoma* and those of cyanobacteria and plastids as well as algal and plant genes rather than with those of other eukaryotic lineages can be explained by the fact that some ancestors of trypanosomes housed in endosymbiont prokaryotes from which a number of genes was then acquired by the nucleus of the trypanosome. Some enzymes of the glycolytic pathway and other pathways seem very close to those found in cyanobacteria and plastids [21].

The sequence of 6PGDH from different species, have been aligned using the programs MultAlin [36] e ESPript [37] to show the conserved amino-acids among species. Of the 482 amino-acids that belong to one subunit, 88 are conserved in all species (Figure 5) [46].

### **5.b) The 3-dimensional structure**

The 3-dimensional structure of the *T. brucei* 6-phosphogluconate dehydrogenase has been solved at 2.8 Å resolution [22]. The sheep liver enzyme, which has 97% sequence identity to the human enzyme, has been described at 2 Å [47] resolution and enzyme-coenzyme and enzyme-substrate complexes have been reported at 2.3 Å -2.5 Å resolution [39]. The structures of *Lactococcus lactis* 6PGDH in ternary complex with NADP and the product Ru5P or the inhibitor 4-phospho-D-erythronohydroxamic acid (PEX) were also reported [48].

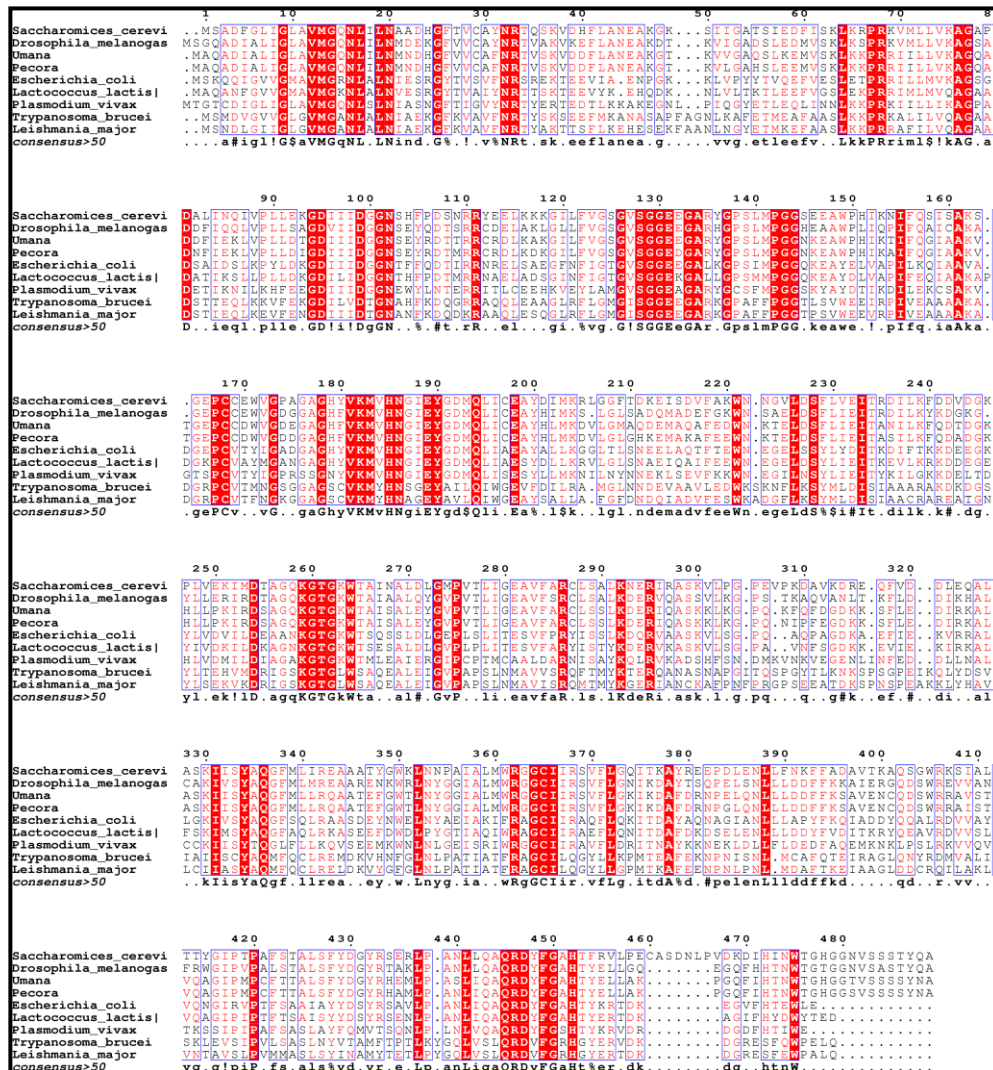


Figure 5. Multiple alignment of 6PGDH from several species.

### 5.c) The *T.brucei* monomer

Each monomeric subunit weighs 52 kDa and it is formed by 482 amino acid residues. The *T. brucei* monomer is comprised of three domains or regions (Figure 6):

[An N-terminal domain or coenzyme binding](#) (residues 1-178), characterized by a Rossmann fold typical for binding to dinucleotides (residues 1-130, sheets from  $\beta A$  to  $\beta F$  alternating with intervening helices) and a unit  $\alpha$ - $\beta$ - $\alpha$  (residues 132 to 161,  $\alpha$ - $\beta$ G- $\alpha$ ) with a section  $\beta$ G antiparallel to the first six strands. The coenzyme binding site is at the carboxyl ends of the strands of the parallel sheet, with the two ribose moieties and the bisphosphate straddling the sheet. The dinucleotide binding fingerprint, at the tight turn following  $\beta A$ , is GxGxxG in the *T. brucei* enzyme while in the ovine enzyme it is

GxAxxG as in almost all known 6PGDHs. As the two subunits of the *T. brucei* dimer were not crystallographically equivalent, slightly different conformations of two loops in the coenzyme domain could be seen [39].

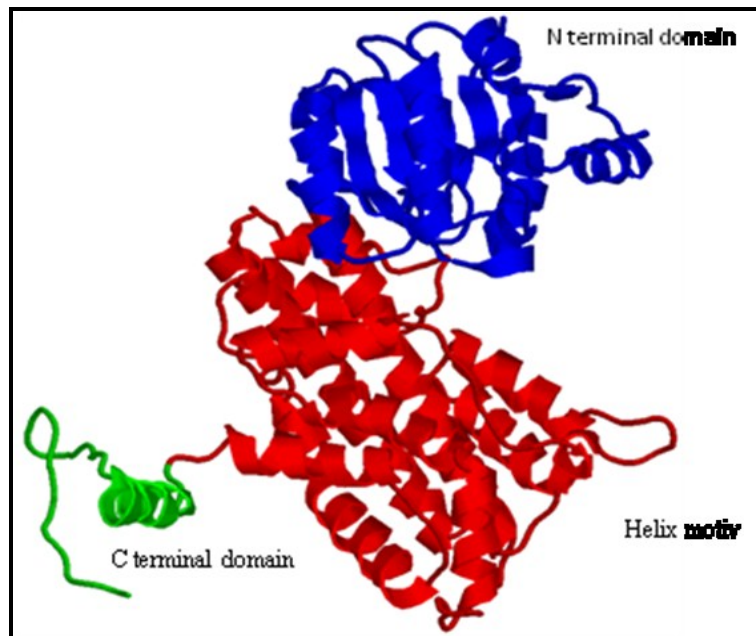


**Figure 6:** Monomer of the *T. brucei* 6PGDH.

Central helical domain "all helix" (residues 179-441) that includes most of the protein, formed only by alpha helices; it forms a part of the interface of the dimer and the binding site to the substrate.

C-terminal "tail" (442-478), of small dimensions which penetrates the central domain of the second subunit, thus completing the binding site to the substrate. (Figure 6).

#### **5.d) Coenzyme binding-site**

The coenzyme binding domain of 6PGDH has 70 residues identical in the sheep and *T. brucei* enzymes (Figure 7), 35 of which are totally conserved.



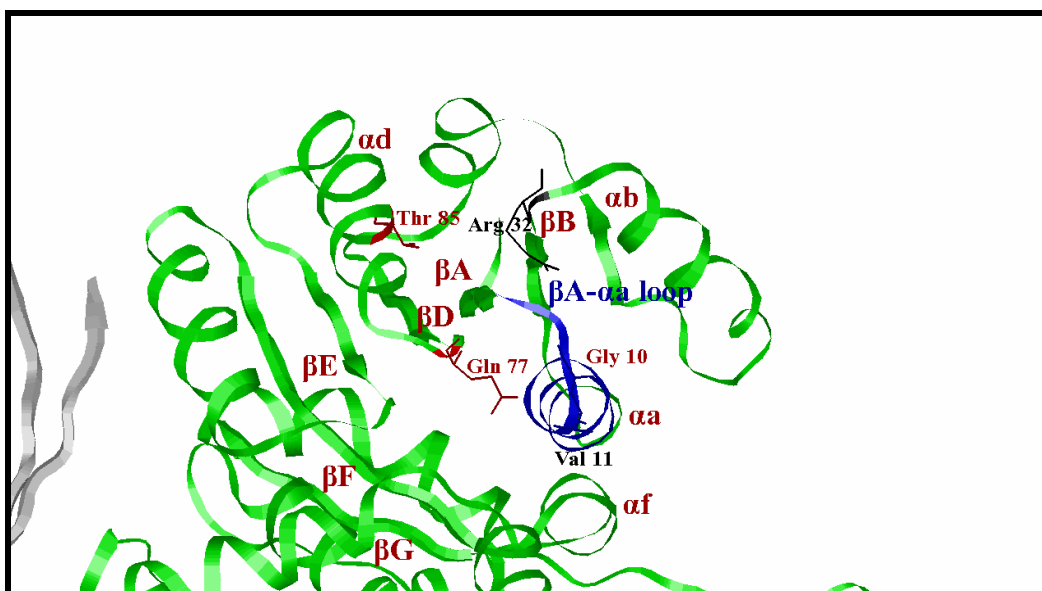


Figure 7. Coenzyme binding site

In the oxidized coenzyme binding site, there are 17 residues within 4 Å from the oxidised coenzyme analogue, nicotinamide-8-bromo-adenine dinucleotide phosphate (Nbr<sup>8</sup>ADP<sup>+</sup>) 6 of which are totally conserved and 12 are identical in *T. brucei* and sheep.

The  $K_m$  for NADP<sup>+</sup> for *T. brucei* 6PGDH is 1 μM while that for sheep enzyme is several times higher ranging from 5.7-8.9 μM depending on pH and ionic strength [49]. Sequence differences at the coenzyme binding site may affect the affinity for NADP<sup>+</sup> between species.

Thus, although most of the binding site is highly conserved, however, some small difference exists. Between these, the most important are the transformation of Ala 11 (sheep) in Gly 10 (*T. brucei*), of Lys 75 (sheep) in Gln 77 (*T. brucei*); and Phe 83 (sheep) in Thr 85 (*T. brucei*) [21]. The mean main-chain movement for the 17 residues of the sheep enzyme on binding the analogue is 0.31 Å; only Lys 75s moves significantly (0.77 Å).

Among the hydrogen bond interactions of the sheep enzyme with oxidised coenzyme, that of the 2'-phosphate and adenine ribose to triplet Asn 32s, Arg 33s, Thr 34s directly following βB (Asn 31, Arg 32, Thr 33 in *T. brucei*) is predominant. The additional hydrogen bonds are to the nicotinamide amide function from a conserved methionine of the fingerprint (Met 13s) and from a glutamate of αf (Glu 131s) conserved in 68 of 70 species. All residues with side-chain hydrogen bonds are conserved between sheep and *T.*

*brucei*, though it should be noted that, in two other species, a tyrosine replaces the arginine 32, (33s), which interacts with the 2'-phosphate. The most important changes in sequence between the sheep and *T. brucei* enzymes, which may affect binding are Ala 11s to Gly 10, Lys75s to Gln 77 and Phe 83s to Thr 85. The C $\beta$  of Ala 11s in sheep 6PGDH protrudes into the bis-phosphate binding site. This residue corresponds to the central glycine of the generic fingerprint; the very small number of direct interactions of the bis-phosphate to the protein is almost certainly a consequence of this alanine. The substitution of glycine for alanine in the *T. brucei* enzyme should allow direct interactions between the enzyme and the NADP<sup>+</sup> bis-phosphate and has a further consequence in that the highly conserved valine 11 (Val 12s) faces towards the putative nicotinamide site in *T. brucei* 6PGDH and away from it in the sheep enzyme. Val 11 would provide further Van der Waals contacts for the nicotinamide ring. The substitution of Gly 10 in the *T. brucei* enzyme would suggest a tighter binding of coenzyme as reflected in the higher affinity.

All links between the 6PGDH side chains and the coenzyme are highly conserved in different species.

Site-directed mutagenesis experiments in which the residue Arg 33 was mutated to tyrosine have revealed the importance of this residue in the binding of 2'-phosphate, which differs in the NADP compared to NAD [51].

As the two subunits of the *T. brucei* dimer were not crystallographically equivalent, slightly different conformations of two loops in the coenzyme domain could be seen [39]. Crystallographic symmetry precludes such observations in the sheep liver enzyme.

Structural studies on the ternary complex of the *E. coli* enzyme have shown that significant conformational changes of this site are required to open the binding pocket at the entrance or release of the coenzyme. Comparing the conformations of the catalytic sites of the two subunits of the enzyme, it seems that while one is in the conformation "open", the other is in the conformation "closed", suggesting that the two subunits are working one at a time, consistent with the mechanism of "half -of-the-site reactivity" of the enzyme induced by the substrate [50]. Other conformational changes at the level of this domain occur following the reduction of the coenzyme.

### 5.e) The dimer interface

Although the interface of the dimer is highly conserved, with 106 of the 134 residues involved, which in the enzyme of the parasite are structurally equivalent to those of sheep, only nine of them have a major role in the formation of the dimer. Three of these residues are part of the domain of the tail. In the enzyme of *T. brucei* the monomer-monomer contact area is of 6210 Å<sup>2</sup> while in that of sheep is of 5488 Å<sup>2</sup> and the interface of the dimer in *T. brucei* presents a greater number of hydrophobic side chains (66 of 134 compared to 49 of 115 of the sheep enzyme).

However, the most notable difference occurs at the point where the tail of a monomer crosses the other helping to form the binding site to the substrate. The tail of the enzyme of *T. brucei*, unlike the sheep one, is full of charges, positive and negative: 13 out of 37 residues are aspartate, glutamate, histidine, lysine and arginine in *T. brucei*, while only 7 of 48 are charged in sheep. Of these 13 charged residues present in *T. brucei*, 5 form inter-subunit salt bridges: two at the coenzyme binding domain and three in the helical domain. None of these salt bridges are conserved among different species. Instead two charged residues, Arg 453 and His 459, highly conserved, interact with sulphate ions firmly bound to the active site [22]. These differences at the level of the queues might be susceptible to drug-targeting [21].

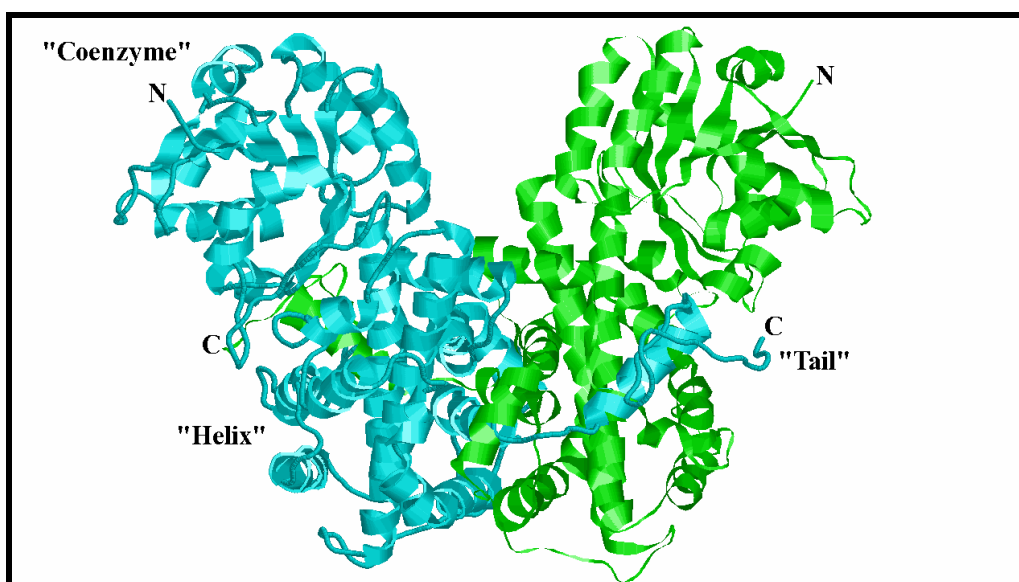


Figure 8. Dimer of the *T. brucei* 6PGDH. The two subunits are drawn in blue and in green.

### 5.f) Substrate binding site

The binding site to the substrate consists of 19 residues within a distance of 4 Å from the substrate 6PG: Asn 104 -102s (the sheep numbering is denoted by a lower case s), Ile 129 - Val 127s, Ser 130 - 128s, Gly 131 - 129s, Gly132- 130s, Lys185 - 183s, His 188-186s, Asn 189 - 187s, Glu 192 - 190s, Tyr 193-191s, Ser 261- Gln 259s, Lys 262 -260s, Gly 263-261s, Thr 264- 262s, Arg 289-287s, Ile 373- 366s, Arg 453-446s, Phe 456- 449s, His 459-452s (figure 9).

Of these, 14 are conserved residues in all species studied: five residues from the domain of the coenzyme, eleven from the helical domain and three from the tail of the second subunit. Of particular importance is the triad S128 - H186 - N187, which turns out to have a multifunctional role in 6PGDH. Site-directed mutagenesis experiments have in fact indicated that these residues are involved in precatalytic conformational changes, helping to keep under control the balance between the open and closed conformation of the enzyme in the binding to 6PG (only S128 and H186) and to NADPH (all three).

The conserved lysine (Lys 183s, Lys 185) predicted to be the base in the reaction is on  $\alpha h$ ; the five residues in this helix, which interact with substrate, have moved less than 0.5 Å in the *T. brucei* 6PGDH compared to the sheep structure.

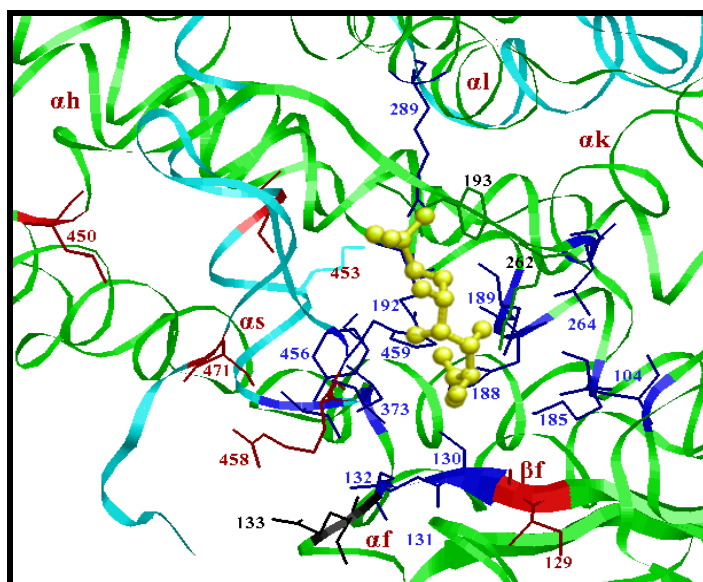


Figure 9: Substrate binding site.

Of particular importance is the Arg 446 (equivalent to Arg 453 of *T. brucei*) that binds the 6-phosphate of the substrate.

The N $\eta$  1 of Arg 446s (Arg 453) is a ligand to the 6-phosphate of 6-phosphogluconate. In the sheep enzyme Arg 446s is oriented by a hydrogen bond from its N $\epsilon$  to the O $\epsilon$ 1 of Gln 443s (equivalent to Ser 450 in *T. brucei*), while Gln 443s N $\epsilon$ 2 interacts with the carbonyl of Gly 258s (equivalent to Gly 260 in *T. brucei*).

Residue 443s is therefore important in constraining the movement of Arg446s and defining the orientation of the phosphate of 6PG. In *T. brucei* 6PGDH, the hydroxyl of Ser 450 hydrogen bonds to the main-chain carboxyl oxygen of Arg 258, but there is no interaction with Arg 453. Arg 458 interacts with the highly conserved Glu 133 (Glu 131s), which should have further implications for interaction with substrate since the carboxyl oxygens of 6PG interact with residues of the  $\beta$ F- $\alpha$ f turn (130- 132, 128s- 130s). These residues have moved almost 1 Å from their position in the sheep enzyme; the movement is correlated with the differing inter-domain hinge angles.

Despite the conservation of first neighbours to 6PG, these changes provide means by which the affinity for substrate and substrate analogues may vary between species, and suggest possible targets for substrate analogue and potential drug interaction.

Additionally, in relation to the Arg 447 of *L. lactis* (equivalent to Arg 446 of sheep) site specific mutagenesis experiments of this residue mutated into Lys (with conservation of charge but size reduction), into Ala (with loss of charge), into Asp (with inversion of the charge) and Trp (with addition of an aromatic group) have confirmed that this residue plays a key role in the activity of the enzyme [52].

Analysis of the structure revealed that, despite the structures of sheep and *T. brucei* 6PGDHs are overall similar, alterations in specific residues involved in binding to the coenzyme, and structural differences that affect the way with which the enzyme binds the substrate, can be used for the development of selective inhibitors for the 6PGDH of *T. brucei* [21].

## 6) Action mechanism of 6-phosphogluconate dehydrogenase

### 6.a) The two key residues

Two residues, one acting as an acid and the other as a base are postulated to assist all the three catalytic steps of the reaction: dehydrogenation, decarboxylation and keto-enol tautomerization. These residues, which in the *T. brucei* enzyme are Glu-192 and Lys-185, have been identified on the basis of crystallographic evidence and site-directed mutagenesis [27-28].

The lysine residue is thought to be protonated in the free enzyme and unprotonated in the enzyme-substrate complex, where it has to receive a proton from the 3-OH of 6PG as a hydride is transferred from C-3 of 6PG to NADP (Figure 3).

The resulting 3-keto-6PG intermediate is then decarboxylated to form the enediol of 5-phospho-ribulose. At this stage an acid, which is thought to be the same Lys-185, is required to donate a proton to the C-3 carbonyl group of the keto intermediate to facilitate decarboxylation. Both a base and an acid are needed in the tautomerization of the enediol intermediate to yield the ketone ribulose 5-phosphate product, with the acid (Glu-192) required to donate a proton to the C-1 of the enediol intermediate and the base (the same Lys-185) accepting a proton from its 2-hydroxyl (figure 3, and figure 10). At the end of the reaction, the protonation state of the two catalytic groups is the opposite to that at the beginning of the reaction; thus an intramolecular proton transfer is required for another cycle of enzyme activity.

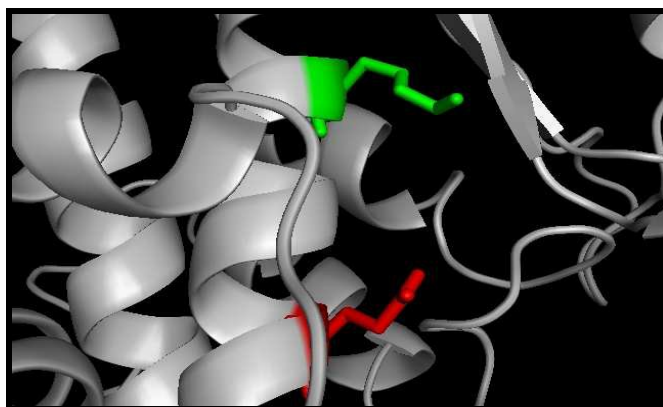


**Figure 10:** *T. brucei* 6PGDH active site with the position of the two residues, discussed in the introduction.

## 6.b) Allosteric modulation by the substrate

### 6.b.1 Asymmetry

6PGDH is a homodimer, but, in many species, it shows functional and structural asymmetry [29- 30]. For instance, both the yeast and sheep liver enzyme bind covalently two molecules of periodate-oxidized NADP, but, in the presence of 6PG, a half-site reactivity is acquired with only one subunit binding the NADP analogue (Figure 11). The *T. brucei* 6PGDH also binds only one 3-amino-pyridine adenine dinucleotide phosphate (aPyADP) per dimer, in the presence of the substrate. NADP inhibition, at low 6PG concentrations, can also be explained by the fact that at low substrate concentration, equilibrium is shifted to the enzyme-(NADP)<sub>2</sub> inactive form, incapable of binding the substrate, while at high substrate concentrations the equilibrium is shifted towards the enzyme-substrate active form [31]. Also 6PGDH from human erythrocytes shows a half-of-the-sites reactivity, indeed it is able to bind two molecules of NADP, but only one of NADPH, and together with rat 6PGDH presents negative cooperativity for NADP. Furthermore, stopped-flow experiments with the sheep enzyme have indicated in the first turnover the formation of only one NADPH molecule per enzyme dimer [32].

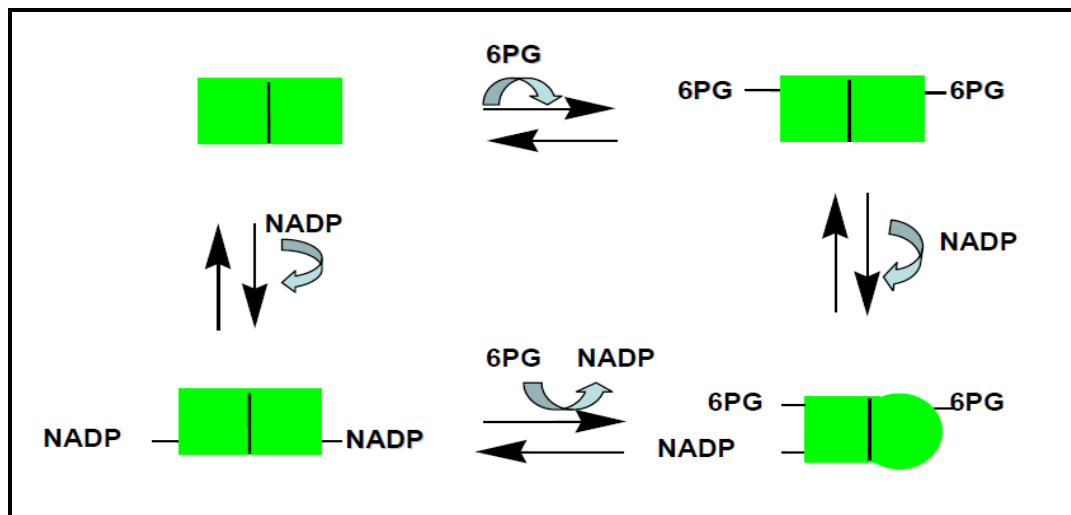


**Figure 11:** Half of the site mechanism. In the presence of the substrate, modification of one of the two NADP binding sites precludes the capability of binding NADP to the corresponding site belonging to the other subunit. These experiments suggest that when one subunit is involved in the ternary complex enzyme-6PG-NADP, the other subunit is unable to bind NADP and is thus inactive

### *6.b.2 Other 6PG-induced effects*

An other significant 6PG effect is the activation of the decarboxylation reaction of 3-keto 2-deoxy 6PG, an analogue of the reaction intermediate 3-keto 6PG, consistent with asymmetry and better with an alternating site co-operativity model (Figure 12), since each subunit has only one substrate binding site. This model foresees that the two enzyme subunits have an alternating role in the oxidative decarboxylation: while one of the two equal subunits catalyses the redox reaction, the other subunit, with a different conformation, catalyses the decarboxylation and tautomerization reactions. Then the two subunits alternate their conformation and role. Both subunits are simultaneously active, participating in different steps of the reaction cycle and inverting the roles. According to this hypothesis while one of the two subunit binds the substrate, the other is involved in the decarboxylation of the intermediate 3-keto-6PG, which is accelerated by conformational changes induced by the binding of the substrate on both subunits. An alternative, less likely, hypothesis foresees the dimer with one permanently catalytic subunit and the other with only a regulatory role; in this case the turnover number would be lower [37].

The substrate binding site is made up of residues from both subunits, allowing the communication between the two active sites [38].

In the presence of either 6PG or phosphate or sulphate, the activity of 6PGDH is much more stable against inactivation by seven proteolytic enzymes, acid, heat, cystamine, DTNB, urea, SDS [33], and different inactivating chemical reagents [34,35-36]. In presence of phosphate buffer the order of binding of 6PG and NADP to the enzyme is different than in triethanolamine buffer [31] and in the presence of 6PG the reactivity of several 6PGDH thiol groups with DTNB is reduced [45]. Again, 6PG increases the reactivity with periodate-oxidized NADP [37,29].



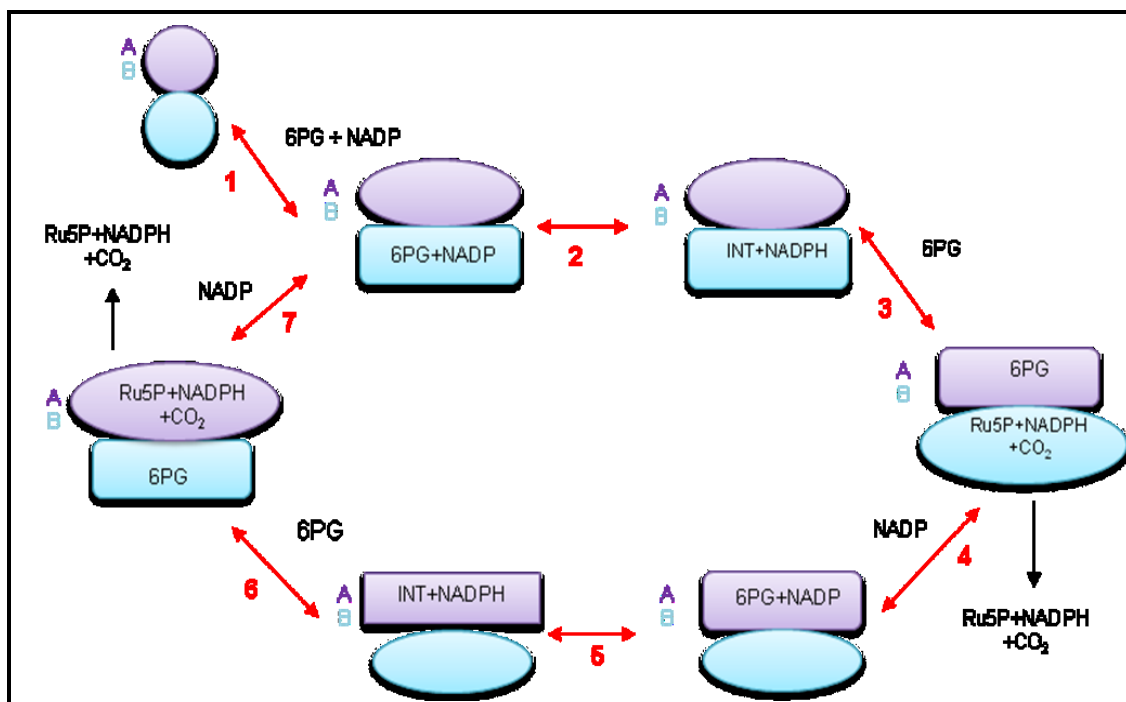


**Figure 12:** Alternating site co-operativity model for the enzyme 6PGDH. "INT" is the reaction intermediate after the redox reaction while "Ru5P" represents both the enolic and the ketonic form of ribulose-5-phosphate. According to this hypothesis, 6PG binds to one (B) of the two structurally equal subunits, inducing in both a different conformational change (step 1). Also NADP binds to the same subunit. Subunit B catalyzes (step 2) the redox reaction producing the intermediate and NADPH. Now 6PG binds to subunit A (step 3) inducing in both subunits a conformational change which promotes subunit B to catalyze the decarboxylation of the intermediate. The reaction goes on, till the products release, then at the binding of NADP to subunit A (step 4), in the A subunit another cycle begins, with the redox reaction (step 5) producing NADPH and the intermediate. The steps 6 and 7 are a repetition of phase 3 and 4, but the subunits have the roles reversed.

### 6.b.3 Isomerization and allostery

$^2\text{H}$  and  $^{13}\text{C}$  isotope effects have shown the both dehydrogenation and decarboxylation steps are partially rate limiting, whereas solvent isotope effects have highlighted a kinetically significant isomerization step preceding dehydrogenation, which is also partially rate-limiting [ 56; 57; 58].

Even in the reverse reaction an isomerisation step preceding the chemical steps is partially rate-limiting but 6PG is able to allosterically activate the reaction, by increasing the affinity for the Ru5P [74]

### 6.b.4 Other significant effects along the reaction

Binding of 4-phospho-D-erythronate (4PE) decreases the dissociation constant of the coenzymes by two orders of magnitude. In a similar manner, the  $K_d$  value of 4PE in the

presence of the coenzymes decreases by two orders of magnitude till 18 nM. The results suggest that 4PE mimics the transition state of dehydrogenation and that 6PGDH undergoes other significant conformational changes along this step of the reaction [19].

However crystallographic data do not show any significant conformational change upon binding of substrate or coenzyme. Instead, all data before described indicate that the binding of the substrate and intermediates modifies in part the conformation of the enzyme in solution, making it, perhaps, more rigid.

All the crystallographic data were obtained with crystals prepared in ammonium sulphate. In the crystals each enzyme subunit has firmly bound three sulphate ions[39]; each of these ions bridges different segments of the protein chain in the same or in a different subunit stabilizing the conformation of the enzyme. Two of these sulphates bind to the active site and one is displaced by 6PG. The finding that the enzyme in the crystals does not show conformational change in presence of 6PG could be due to the fact that these changes were already induced by bound sulphates.

---

# *Aim of the Thesis*

The aim of the thesis is to acquire functional and structural information suitable for a more efficient design of inhibitors for 6PGDH from *T. brucei*.

The thesis is divided into two parts, which concern, the first, about structural studies on *T. brucei* 6PGDH, and, the second, about functional studies on the enzyme.

## **1) Structural studies**

Much discrepancy exists between the fixed crystallographic picture of 6PGDH and the ligand-induced significant properties of the enzyme. For instance, overlays between the X-ray structures of 6PGDH alone and in binary complexes with either 6PG or coenzymes result in a r.m.s.d. of 0.22 Å for C<sup>α</sup> and 0.6-0.7 Å for all atoms, suggesting that ligand binding does not modify enzyme conformation. Nevertheless, compared to free enzyme, the enzyme-6PG complex shows lower reactivity toward chemicals, denaturing agents and proteolysis, and many other evidences exist on significant conformational changes induced by 6PG (see introduction). Some studies of the past years suggested that the *T. brucei* 6PGDH might undergo an oligomerization process on particular conditions. One objective of the thesis is to study in depth this phenomenon by means of several experimental approaches:

- \* gel filtration
- \* crosslinking with glutaraldehyde
- \* dynamic light scattering (DLS)
- \* sucrose density gradient centrifugation
- \* isothermal titration calorimetry (ITC) studies.

## **2) Functional studies**

One important information that cannot be obtained from X-ray structures is the protonation state of the ionisable residues present in a specific site. After a catalytic cycle, *T. brucei* 6PGDH requires an intramolecular transfer of a proton. In fact at the end of the reaction Lys 185 should become protonated and Glu 192 unprotonated; but for a new catalytic cycle

is necessary that lysine is unprotonated and glutamate protonated. Hence an other objective of the thesis is to explore the ionisation state and the  $pK_a$  of Lys 185 and Glu 192 in the free enzyme and in the enzyme-substrate complex, by the combined use of site-directed mutants and ITC studies. We further explored the ionisation state of His 188 which is a conserved residue at 4-5 Å from Glu 192.

---

# MATERIALS AND METHODS

## 1) Site-Directed Mutagenesis

We used the technique of site-specific mutagenesis to obtain mutants of interest. (K185H; E192Q and H188L) by changing a single nucleotides triplet in the gene of *T. brucei* 6PGDH, cloned in the vector of expression pET3a (double-stranded). The complete plasmid is called pT7gnd. The plasmids extraction was from bacterial stock JM109 (genotype: F '[traD36, proAB +, lacIq, lacZD (M15)], recA1 ednA1 gyrA96 thi hsdR17 supE44 relA1 D (lacproAB).

The stock JM109 has been used for cloning of the gene of the wild type enzyme. Quick Change II site-directed mutagenesis kits were used (Stratagene) (Figure 13).

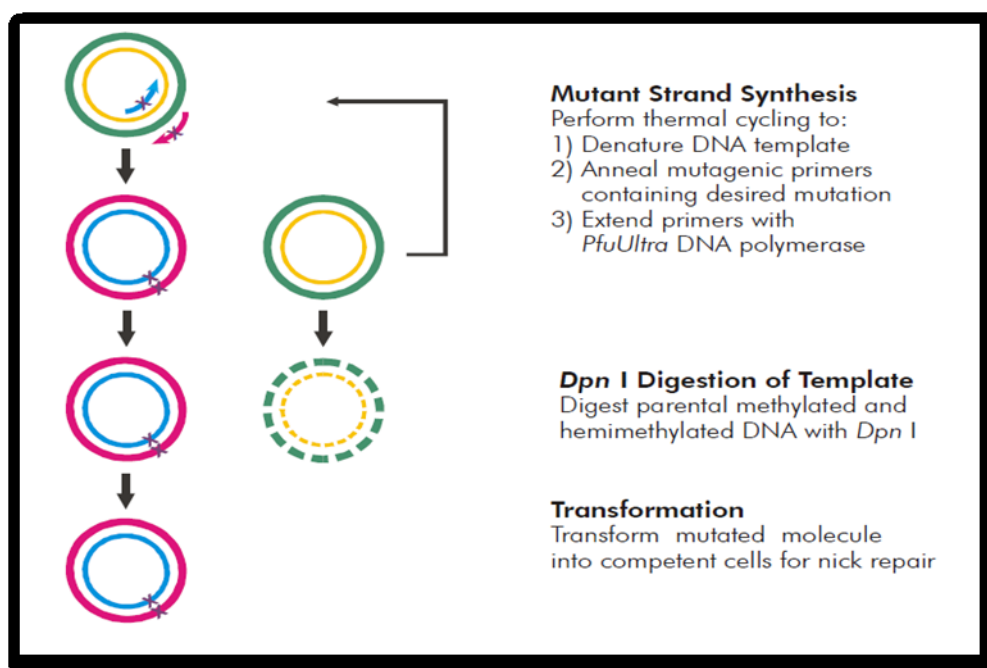


**Figure 13:** Scheme of the QuickChange II site-directed mutagenesis method.

Mutagenesis was conducted in a double-stranded vector DNA, which was denatured to allow the pairing of oligonucleotides with small sequences of the 6PGDH gene of *T. brucei* containing the mutation of interest. (Table 3).

K185H 5'	GGATCATGCGTGCATATGTACCACAATTCG	3'
E192Q 5'	GATGTACCACAATTCGGGTCAATACGCCATTTTGCAAATCTG	3'
H188L 5'	GGCGTATTCACCCGAATTAAGGTACATCTTCACGCATGATCCC	3'

**Table 3.** Primer oligonucleotides synthesized by MWG-biotech AG.

For each mutation two primers were used, complementary to opposite strands of the vector, both containing the desired mutation. With dNTP and a PfuUltra™ High Fidelity (HF) DNA polymerase two new chains are synthesized, generating plasmids bearing the mutation, containing "nicks" arranged at intervals (Table 4). The temperature cycling used is indicated in Table 5.

reaction buffer (10X) 5µl
dsDNA template (5 -50 ng) 2 µl
Forward Oligonucleotide (125 ng) 12.5 µl
Reverse Oligonucleotide (125 ng) 12.5 µl
dNTP mix 1 µl
ddH2O to a final volume of a 50 µl
di <i>PfuTurbo</i> DNA polymerase (2.5 U/µl) 1 µl

**Table 4:** The protocol reaction

Segment	Cycles	Temperature	Time
1	1	95 C°	30 seconds
2	12-18	95 C°	30 seconds
		55C°	1 minute
		68C°	1 minute/kb of plasmid length

**Table 5:** The temperature cycling

After primer extension, the reaction mixture was placed on ice for 2 minutes to cool to  $\leq 37^{\circ}\text{C}$ .

The vector filament moulds were removed using *Dpn I* endonuclease (target sequence: 5'-Gm6ATC-3') which is able to digest the methylated and hemimethylated DNA (the DNA isolated from almost all strains of *E. coli* is methylated). In this way only the newly synthesized DNA containing the mutation was selected. *Dpn I* endonuclease (10U/ $\mu\text{l}$ ), was mixed with the reaction solution gently by pipetting the solution. The reaction mixtures are then spun down in a microcentrifuge for 1 minute and immediately incubated at  $37^{\circ}\text{C}$  for 2 hours to digest the parental supercoiled dsDNA.

Finally mutated carriers must be repaired by removing the "nicks" and amplified. Therefore, the vectors containing the desired mutations were transformed into XL1-Blue supercompetent cells. The supercompetent cells are gently thawed on ice, for each sample reaction to be transformed an aliquot of 50  $\mu\text{l}$  were put in a tube and 1  $\mu\text{l}$  of the *Dpn I*-treated DNA is transferred. The transformation reactions were gently swirled and incubated on ice for 30 minutes, then heat pulsed for 45 seconds at  $42^{\circ}\text{C}$  and after placed on ice for 2 minutes. 0.5 ml of NZY+ broth preheated to  $42^{\circ}\text{C}$  was added (NZY+ broth: 10g of NZ amine, 5g of yeast extract, 5g of NaCl, 12.5 ml of 1 M  $\text{MgCl}_2$ , 12.5 ml of 1 M  $\text{MgSO}_4$  and 20ml of 20% (w/v) glucose per liter, adjusted to pH 7.5).

The transformation reactions were then incubated at  $37^{\circ}\text{C}$  for 1 hour with shaking at 225-250 rpm. 250  $\mu\text{l}$  of each transformation reaction was plated on agar /antibiotic, then put at  $37^{\circ}\text{C}$  for > 16 hours.

The following steps were the extraction of plasmidic DNA from a single colony and sequencing of the entire coding region of mutants *T. brucei* 6PGDH to check that only the single mutation was present, using the dideoxynucleotide chain-termination method. Once mutated sequence was obtained, it was introduced into *E. coli* strain BL21 (DE3) for inducible expression.

## **2) Overexpression of the *T. brucei* enzyme in *E. coli*.**

PT7gnd is a plasmid obtained from cloning of the gene gnd (encoding 6-phosphogluconate dehydrogenase) into the vector pET3a, with the ATG initiation codon oriented adjacent to the bacteriophage T7 RNA polymerase promoter. BL21 (DE3) are *E. coli* cells with the phage DE3 encoding T7 RNA polymerase under the control of the lacUV5 promoter.

15 ul of transformed bacteria (stored at -80 °C in glycerol) were added to a Petri dish with agar, then left overnight at 37 °C. The next day a single colony was taken and added to 16 ml LB/16 ul amp (Luria Bertani broth plus ampicillin: 10g tryptone, 5 g yeast extract, 10 g NaCl water until 1 liter) and stirred overnight at 37 °C.

The 16 ml of the preculture were added to 400 ml of LB/amp, and incubated at 28 °C with shaking until the culture reached an optical density of 0.6 at 600nm. At this time the inducer IPTG (the lac operon inducer isopropylthiogalactopyranoside) was added to the culture to a final concentration of 0.4 mM. After adding IPTG , cultivation was left at 28 °C under shaking for 4 hours.

Then cells were centrifuged at 4000 rpm for 10 minutes at 4 °C. Pelleted cells were resuspended in buffer TEA (50mM TEA; 0.1 mM EDTA; 1 mM mercaptoethanol, pH 7.5) to a final volume of 20 ml and stored at -80 °C.

## **3) Purification of 6-PGDH wt / mutant of *T. brucei* by bacteria *E. coli***

The recombinant *T. brucei* 6PGDH, overexpressed in *Escherichia coli*, was purified according to a technique that was slightly modified compared to the original of Barrett [2]

After keeping at -80 °C the bacteria were sonicated (XL2020 model sonicator, Heat Systems, power level to 4, 5 short bursts of 10 sec, followed by intervals of 20 sec for cooling, keeping the suspension at all times on ice).

Cell debris and insoluble material were then spun down (40,000 rpm, 30min). The supernatant was applied to a 15 ml DEAE-Sepharose column equilibrated with TEA



buffer, which was then washed with the same buffer and the flow through material absorbing at 280 nm was loaded directly onto a 5 ml 2',5'-ADP-Sepharose column, equilibrated with TEA buffer diluted 10 x.

After washing with the same buffer, the enzyme was eluted with sodium pyrophosphate ( $\text{Na}_4\text{P}_2\text{O}_7$ ) 150 mM containing 1mM EDTA pH 7.2 and the specific activity assayed in buffer containing 0.6 mM 6PG and 0.26 mM  $\text{NADP}^+$ .

The whole purification lasted less than one day and was monitored both by SDS-PAGE and activity assays. Enzyme was stored in the presence of 50% glycerol at  $-20^\circ\text{C}$ .

#### **4) Determination of protein and 6PGDH wt/mutant concentration**

Spectrophotometric measurements were made throughout with a Jenway 6715 or a Kontron Uvikon 930 spectrophotometer or a Tecan infinite 200 microplate reader. Protein fluorescence was measured with the same microplate reader.

The protein purification fractions were measured spectrophotometrically at a wavelength of 280 nm for determination of the protein concentration assuming that a solution containing 1mg/ml of protein have an absorbance of 1 O.D. A solution containing 1 mg/ml of pure 6PGDH has instead at 280 nm an absorbance of 1.023. Knowing that each monomer unit of the *T. brucei* 6PGDH weights 52 kDa we can calculate that 1 mg of protein contains 19.2 nmoles. Therefore 1 mg/ml of the enzyme corresponds to a 19,2 microM concentration having an absorbance at 280 nm, 1.023 O.D.

To facilitate the storage of samples, the fractions were concentrated by the technique of ultrafiltration using Amicon Ultra-15 Centrifugal Filter Devices (Millipore) at 4000 rpm. The concentrated samples are assayed for the concentration and stored in 50% glycerol at  $-20^\circ\text{C}$ .

## **5) Enzyme activity. Assay of activity for 6PGDH**

The assay is based on the measurement of kinetics of a reaction mixture containing the 6PG substrate (0.6 mM), the NADP cofactor (0.26 mM) and our enzyme at a proper dilution; in 50 mM TEA buffer with 0.1 mM EDTA at pH 7.5, we proceeded to measure at a wavelength of 340 nm the amount of NADPH produced (product of the reduction of the cofactor NADP.) The absorbance value is divided by the molar extinction coefficient of NADPH which is 6,220.

The international unit of enzyme activity (IU) is the amount of enzyme which catalyzes in one minute, the formation of one micromol NADPH in standard conditions (25 °C and pH optimum). The specific activity of the enzyme has been calculated as the number of UI divided by the number of mg of protein.

## **6) Cysteines reactivity**

The method G. Ellman reaction, [59] is based on the capacity of sulphidrilic groups of cysteines to react with 5,5-ditiobis-2-nitro benzoic acid (DTNB), developing a spectrophotometrically measurable complex at the wavelength of 412 nm. The method is rapid and the stoichiometry is 1:1, coloured product : thiol. Before the reaction, enzyme is freed from glycerol, by gel-filtration or dialysis, and used at a concentration 6 microM. DTNB is used at a concentration of 4 mg/ml and prepared in natrium phosphate buffer 0.2 M. Labelling has been measured for 45 min. The product molar extinction coefficient is 13,600.

## **7) Polyacrylamide gel electrophoresis (SDS-PAGE)**

The polyacrylamide electrophoresis was performed following the method described by Laemmli [60] using a 8 x 10 cm gel in a socket for vertical electrophoresis.

The electrophoretic technique involves the preparation of two mixtures: one for the stacking gel which is at the top of the complete gel, in which the concentration of

acrylamide is 5% (w/v) and pH 6.8, and the second for the running gel which is under the stacking gel, in which the acrylamide concentration varies depending on the chosen pore size and the pH is 8.8. The running gel is the gel where protein separation is performed. In our case the acrylamide concentration used was 10% to verify the purification of the enzyme while both 10 and 7.5% for cross-linking experiments.

### **Running Gel (10%)**

1.5 ml of 40% acrylamide buffer (39.3% acrylamide, 0.7% methylenbisacrylamide)

1.5 ml of TrisHCl (Tris-hydroxymethyl-aminomethane) 1.5 M pH 8.8,

15 µl of 6.6 M TEMED (N, N, N', N'-tetramethylethylenediamine)

2.9 ml of water

60 µl of SDS (sodium dodecyl sulphate) 10% w/v,

30 µl of ammonium persulphate 10% w/v.

### **Running Gel (7,5%)**

1.125 ml of 40% acrylamide buffer (39.3% acrylamide, 0.7% methylenbisacrylamide)

1.5 ml of TrisHCl 1.5 M pH 8.8,

15 µl of 6.6 M TEMED

3.26 ml of water

60 µl of SDS 10% w/v,

30 µl of ammonium persulphate 10% w/v.

The solution of the running gel was poured between the two glass panes and left to solidify.

In this period it was prepared *the stacking gel* solution 5% (w/v) as indicated in Table 6.

500  $\mu$  l acrylamide buffer 20% (19.6% acrylamide, 0.4% methylenbisacrylamide)

500  $\mu$  l 0.5 M TrisHCl pH 6.8

8  $\mu$  l 6.6 M di TEMED

930 ul of water

20 ul SDS 10% w/v

20  $\mu$  l ammonium persulphate 10% w/v.

**Table 6:** the stacking gel solution 5% (w/v)

The solution of the stacking gel was poured over the polymerized running gel and the spacer comb for the wells was fitted between the two panes. Then the gel was left to polymerize. After, spacer was removed and the gel was installed in the device for electrophoresis, the tray containing the electrodes was filled with running buffer (25 mM Tris, 192 mM glycine, 0.1% SDS, at pH 8.3).

The samples were denatured before to be loaded into the wells. Buffer of denaturation (12.5% v/v 0.5 M Tris pH 6.8, 2% w/v SDS, 5% v/v  $\beta$ -mercaptoethanol, 10% v/v glycerol) containing a small amount of bromophenol blue as a tracer, was added to samples and then these were brought to 90 °C for 4 min. After denaturation 20 $\mu$ l of each sample was applied to the wells of the gel.

The electrophoresis was conducted by applying a current of 25 mA until the tracer had reached the lower limit of the gel, (power supply parameters: 0.46 KV, 25mA, 35 W, 45-50 min).

Since the run was done in the presence of SDS, the samples acquired the same negative charge and the migration is according the relative molecular weight of the sample.

After the run was completed the gel was extracted from the support and stained with Comassie blue C250 coloration without methanol (Table 7).

In 1 liter of bidistilled water
80 mg of Coomassie Brilliant Blue G-250
HCl in 40 mM final concentration.

**Table 7:** Coomassie blue C250 without methanol.

The gel in the dye solution was put in a microwave oven for 2-3 cycles of 15 seconds at maximum power. Then it is left in slow shaking for about 15 minutes at room temperature. Finally, the dye was removed and gel is soaked in distilled water at room temperature, rinsed several times and left in water in gentle agitation. Densitometric analysis of the gel was done with the program Quantity One (Biorad).

## **8) Gel Filtration (Sephacryl S-200 HR and AcA 34)**

In gel filtration chromatography – also known as size exclusion chromatography – separation is based on differences in the size and/or shape of the analyte molecules, which governs the analytes' access to the pore volume inside the column packing particles. The exclusion limit of a size exclusion packing indicates the molecular weight, for a particular polymer type, above which analytes are fully excluded from entering the pores and thus will not be separated. According to their size, smaller analytes have partial to complete access to the pore volume. Larger molecules with less access to the pore volume elute first, while the smallest molecules elute last. The fractionation range means that molecules within that molecular weight range can be separated.

In the study, two gel filtration matrices were used: Sephacryl S-200 from GE Healthcare and ACA-34 Ultrogel from LKB. Sephacryl High Resolution is a cross-linked copolymer of allyl dextran and N,N'-methylene bisacrylamide, which can separate proteins in the molecular weight range  $5 \times 10^3 - 2.5 \times 10^5$  Da. The diameter of the Sephacryl column was 0.7 cm and height 16.5 cm. The flow rate was of 3.3 microl/sec.

ACA-34 Ultrogel is polyacrylamide/agarose with a linear fractionation range of 20-350 kDa and an exclusion limit of 750 kDa for globular proteins. The diameter of the column was 0.8 cm and height 20 cm (7.6 ml of resin). The flow rate was of 210 microl/sec.

Calibrations were performed with aldolase (160 kDa), bovine serum albumin (66 kDa), beta-lactoglobulin (35 kDa).

Columns were equilibrated with 50 mM triethanolamine, pH 7.5, 0.1 mM EDTA and 1.0 mM 2-mercaptoethanol. 20-40 microl of protein at a subunit concentration of 50 microM (about 3 mg/ml) were loaded onto the columns. The effect of ligands was determined by equilibrating the column with 70 microM NADP(H) or/and 0.16 mM 6PG. 4PE was used at 0.16 mM. Ligands were added to the enzyme sample before column loading to the same final concentrations used for the columns or higher. Eluted fractions were collected in opaque-walled plate, with 100 microl/well and a total of 24 fractions. Protein detection was by measure of the protein fluorescence, due essentially to tryptophans, using an excitation wavelength of 280 nm and an emission wavelength of 340 nm. The emission at 340 nm is proportional to the concentration of the sample, in this way we were able to locate the wells containing the eluted sample and create a curve of elution.

## **9) Chemical cross-linking of 6PGDH**

Many biochemical and biophysical methods can be used to characterize the oligomerization state of proteins. One of the most widely used is glutaraldehyde cross-linking. The simplicity of the procedure, which requires only the mixing of glutaraldehyde with the protein solution and the availability of glutaraldehyde as a common reagent easily found in a biochemical laboratory, and the direct detection of cross-linked products by SDS-PAGE have led to the wide application of this method. The major limitation of the technique arises from the non-specificity of the reagent, which can react with all the nitrogens of a protein and mainly with lysines, tyrosines, histidines, and arginines and . Intra- and intermolecular links are formed that could connect atoms of neighboring but not interacting molecules, yielding artificial protein oligomers that lack biological significance. To eliminate the possibility of artificial interactions, the proper reaction conditions must be established through a detailed and often time-consuming investigation of the influence of

many parameters such as protein concentration, reagent concentration, temperature, and time of reaction [61]

Glutaraldehyde is a linear, 5-carbon dialdehyde. It reacts rapidly with amine groups at around neutral pH [62] and is more efficient than other aldehydes in generating thermally and chemically stable crosslinks. [63]. It is a bifunctional reagent because two aldehyde groups can react with two amino groups via Schiff base (Figures 14 and 15). [64]

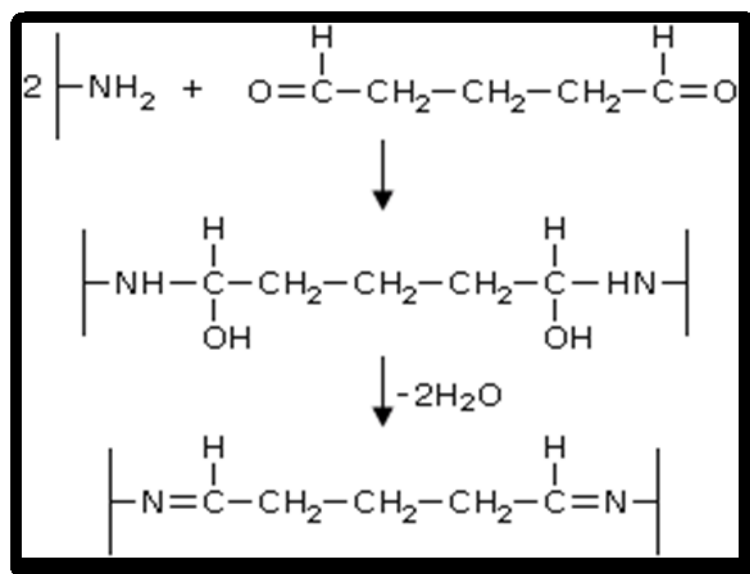


**Figure 14:** Reaction of the amino groups of proteins with glutaraldehyde.

The simple structure of glutaraldehyde is not indicative of the complexity of its behaviour in aqueous solution and its reactivity. The structure of glutaraldehyde in aqueous solution has been the subject of more debate than any of the other crosslinking reagents. In fact, glutaraldehyde structure in aqueous solution is not limited to the monomeric form (Figure 16) [63], it can also undergo intramolecular cyclization, for instance producing pyridines (Figure 15). At alkaline pH polymerization of glutaraldehyde makes possible Michael-type additions with the formation of other types of condensation with amino groups (Figures 15 and 16).

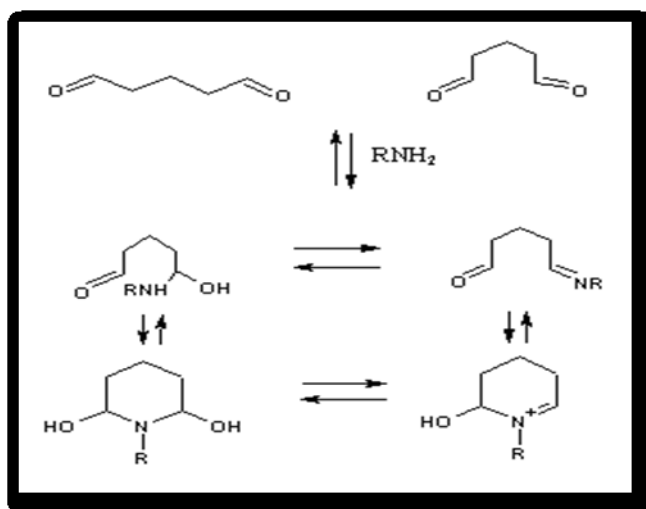


**Figure 15:** Formation of pyridine rings after the reaction of glutaraldehyde with amino groups of proteins.

Glutaraldehyde cross-linking was performed at different concentrations of enzyme and glutaraldehyde. The concentrations range were 0.1-1 mg/ml for the enzyme and 0,05-5 % for glutaraldehyde. Reaction was in 0.04 M sodium pyrophosphate, 25 mM HEPES (pH 7.5), containing 0.5 mM EDTA. Different incubation times (1, 2, 3, 5 minutes) were assayed and the reaction was stopped by adding 40  $\mu$ l of 1 M TRIS/HCl pH 8.0. Aliquots were then resolved by either 7,5% or 10% SDS-PAGE. The more efficient cross-linking condition was with a final 1 % glutaraldehyde (by mixing 0.5 ml of enzyme with 20  $\mu$ l of 25 % glutaraldehyde). Cross-linking was made also in presence of either 40  $\mu$ M NADPH or both 40  $\mu$ M NADPH and 1mM 4PE.

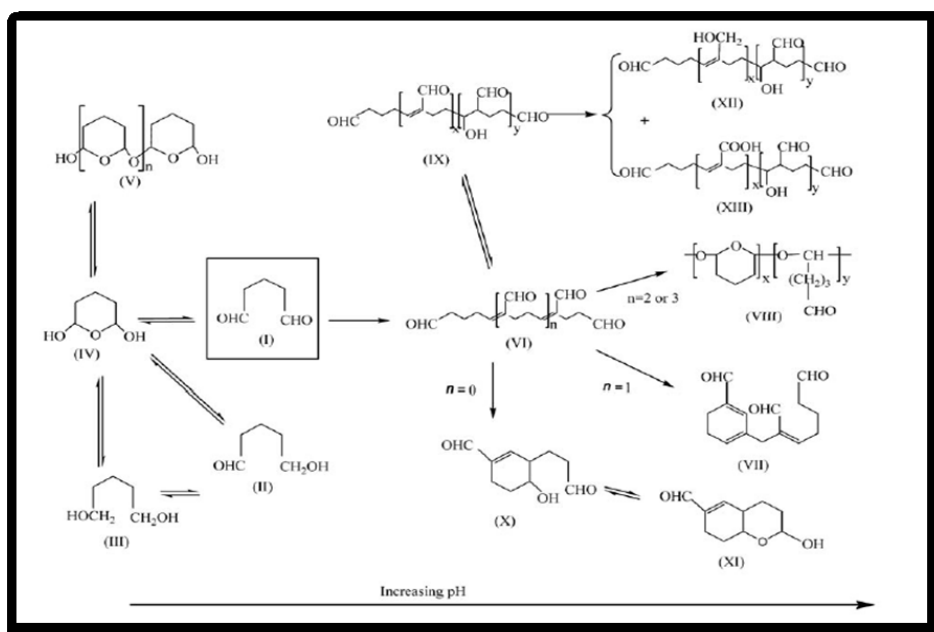


**Figure 16:** Summary of the possible forms of glutaraldehyde in aqueous solution.



## 10) Dynamic Light scattering (DLS) measurements

DLS may be used as a complementary tool for characterization of proteins. This technique is used for measuring the size and size distribution of molecules and particles typically in the submicron region, and with the latest technology lower than 1 nm. [66].

It is a relatively fast method of characterizing the size of biomolecules in solution, taking only minutes for a measurement. It may be used to distinguish between a homogenous monodisperse and an aggregated sample. Quite frequently in nature, oligomeric states exist in equilibrium in solutions of biomolecules [65].

When light passes through a solution containing molecules, depending on the optical parameters of the system, part of the light will be scattered. This scattered light may be analysed either in terms of its intensity or in terms of its fluctuations. The former type of analysis is called static light scattering and may be used to find the molar mass and radius of gyration. However, for many typical biomolecules (< 20 nm), the radius of gyration is not easily measurable since only a minor angular variation in the intensity is exhibited. This means that measurements may be performed at a single angle, provided the concentration and the refractive index are known.

The DLS technique is capable to detect the fluctuations of the scattering intensity due to the Brownian motion of molecules in solution. [67] Thus it measures the diffusion of particles moving under Brownian motion, and converts this to size and a size distribution.

The wave vector determines the length scale over which molecular motions are detected

and it is given by:

$$q = 2\pi n \sin(\theta/2)/\lambda$$

**Equation 1:** The wave vector

where  $n$  is the refractive index of the buffer,  $\lambda$  is the wavelength of the radiation, and

$\theta$  the scattering angle.

In our case (Zetasizer Nano S, Malvern) the light source is He-Ne laser 633nm, allowing a size measurement range 0.3nm – 10.0 microns (diameter) and a molecular weight range 980 Da – 20 MDa.

The dynamic information of the particles is derived from an autocorrelation of the intensity trace recorded during the experiment.

The resulting correlation function is:

$$g^2(q; \tau) = \frac{\langle I(t)I(t + \tau) \rangle}{\langle I(t) \rangle^2}$$

**Equation 2:** Correlation function. of the scattering signal. The correlation is based on the measurement of the intensity in function of time

where  $g^2(q; \tau)$  is the autocorrelation function at a particular wave vector,  $q$ , and delay time,  $\tau$ , and  $I$  is the intensity.

It is expected to show — under ideal conditions — a single exponential decay

$$G(\tau) = 1 + \beta \exp(-Dq^2\tau)$$

**Equation 3:** Equation for single exponential decay for the correlation function G

where the decay rate  $Dq^2$  includes the diffusion coefficient  $D$  of the molecules, and the fitting parameter  $\beta$  is related to the ratio of coherent signal to incoherent noise .

The Stokes-Einstein relation may be used to convert the measured diffusion coefficient (equation 4) into a hydrodynamic diameter  $d_H$  which is the size of a sphere that has the same diffusion behaviour.

$$D = \frac{k_B T}{3\pi\eta d_H}$$

**Equation 4:** The Stokes-Einstein relation used to convert the measured diffusion into a hydrodynamic diameter  $d_H$

In the Stokes-Einstein relation,  $T$  is the absolute temperature,  $K_B$  the universal Boltzmann constant and  $\eta$ , the viscosity of the buffer.

In the end a z-average or cumulant average, particle diameter is recovered. A polynomial fit to the logarithm of the function leads to the size (the first cumulant) and its deviation (the second cumulant), where the polydispersity index PDI corresponds to the square of the normalised standard deviation of an underlying Gaussian size distribution.

Mean hydrodynamic radius measurements were compared with value calculated by the Hydropro software [68]

Measurements were carried out on:

- free enzyme
- binary complex: enzyme-NADPH
- tertiary complex: enzyme-NADPH-4P-erythronate

Measurements were performed at 25 °C or 5 °C.

The measurements were made at the Department of Biochemistry, University of Verona.

The buffer used for measurements was 50 mM Triethanolamine (TEA), pH 7,5 with 0,1 mM EDTA and 1 mM 2-mercaptoethanol, filtered immediately before use to eliminate impurities.

The protein concentration used were 2 and 20 microM. The concentrations of NADPH and 4PE were 0.2 mM and 0.5 mM, respectively.

## 11) Sucrose-density-gradient centrifugation

Sucrose density gradient ultracentrifugation is a powerful technique for fractionating macromolecules like DNA, RNA, and proteins. To this purpose, a sample containing a mixture of different size macromolecules is layered onto the surface of a gradient, whose density increases linearly from top to bottom. During centrifugation, different size macromolecules sediment through the gradient at different rates.

The rate of sedimentation depends, in addition to centrifugal force, on the size, shape, and density of the macromolecules, as well as on the density and viscosity of the gradient. In this way, macromolecules are separated by size with larger ones sedimenting towards the bottom and lighter ones remaining close to the top of the gradient. [69]

Fractionation studies by sucrose density gradient was widely used in the molecular weight determination of proteins.

On top of a 11.2 ml discontinuous sucrose gradient with 5 %, 10 %, 12.5 %, 15 %, 20 % and 35 % (w/v) cushions, 0,1-0.2 ml of sample, free of glycerol, at a concentration of 1 mg/ml was layered and centrifuged at 38,000 rpm for 19 h at 4°C, by using the swing-out rotor SW40 in a Beckman XL-70 ultracentrifuge. Sucrose solutions were prepared with 0.05 M triethanolamine, pH 7.5, with 0.1 mM EDTA and 1 mM 2-mercaptoethanol, with or without ligands.

During every cushion preparation, tubes were weighted till the same weight was reached, then tubes were put at -80°C. The second cushion was stratified onto the first when it was freezed. The centrifuged solution was fractionated into 70 fractions from the bottom, by laminar flow within a subtle flexible plastic tube connected to glass capillaries with a diameter of 1 mm, at the two ends (Figure 17). Some tubes contained, as molecular weight markers, lactate dehydrogenase (140 kDa) and bovine serum albumin (66 kDa). The rotor was decelerated with the brake off.

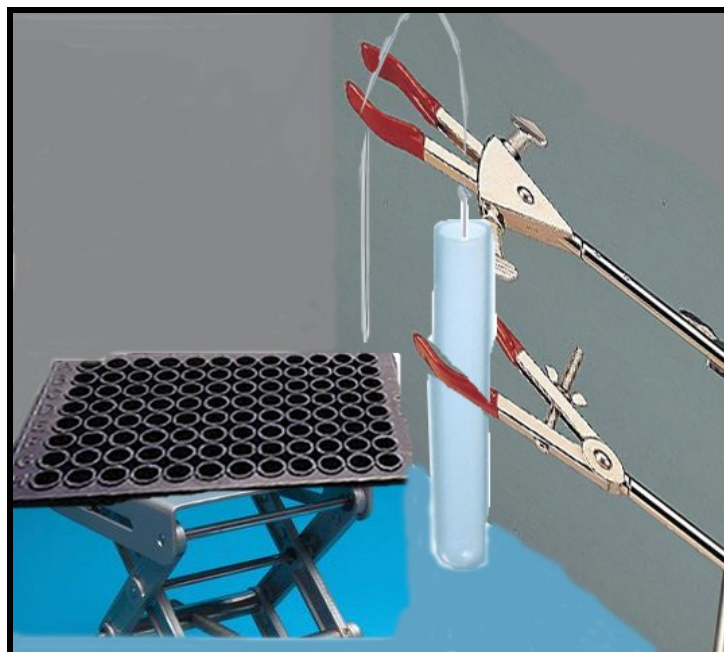


**Figure 17.** : Collecting of the fractions after the density-gradient centrifugation.

## 12) Isothermal titration calorimetry (ITC)

Isothermal titration calorimetry (ITC) is a well established technique that can determine the enthalpy of a binding interaction ( $\Delta H$ ), the binding affinity ( $K_a$ ) and stoichiometry in a single experiment. Also the entropy ( $\Delta S$ ) and free energy ( $\Delta G$ ) changes are detected. ITC works by titrating one reactant with a second reactant under isothermal condition. The signal measured is the heat released or absorbed upon interaction (binding) of the two reactants. A series of injections are performed and the heat signal will approach zero as the limiting reactant becomes saturated. Fitting of the isotherm gives the thermodynamic parameters [70].

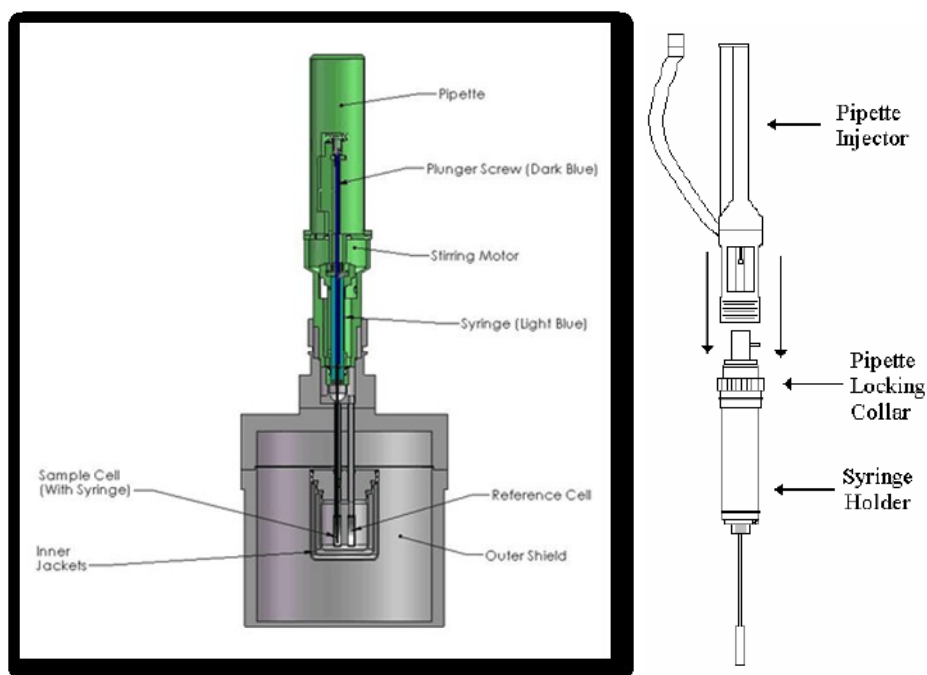
To this end the calorimeter goes to directly measure the heat (released or absorbed) associated with a reaction, which, at constant pressure, is equal to the enthalpy change in this process, the  $\Delta H$ .

When two molecules bind, heat released or absorbed is proportional to the increase in complex concentration. At the end, saturation of the protein is reached and any signal of heat is due to the background noise.

The instrument consists of two identical cells surrounded by an inner shield and an outer one, and an injecting syringe loaded with the solution of one ligand (Figure 18).

These two coatings are maintained at the same temperature of the cells to minimize heat flows from or to the cells. The measurement of the heat released or absorbed is performed by two control systems concatenated, placed both on the cells and on the coats that surround them. The first measures the difference in temperature between the two cells, while the second system measures the temperature difference between the cells and the outer casing. The temperature in the reference and the sample cell is kept identical, subtracting or providing heat to the sample cell. The integral of the power supplied to maintain constant over time  $\Delta T_1$  (the difference in T between the two cells) is a function of the total heat involved in the reaction.

A VP-ITC microcalorimeter (Microcal, Northampton, MA, USA) was used.



**Figures 18 :** Schematic representation of a VP-ITC microcalorimeter and the syringe .

A sequence of injections is programmed and the solution of the ligand periodically is injected in the sample cell.

Because some proteins aggregate at the high concentrations needed for the species in the injection syringe, most often the protein is loaded into the sample cell. The optimal macromolecule concentration is at least 10 fold higher than the predicted affinity of the system, though it is possible to get accurate data for weak-binding systems under specific experimental conditions with concentrations below.

The concentration of the ligand should be large enough (7-25 fold more concentrated than the  $K_d$  for the weakest ligand binding site) so that saturation occurs within the first third to half of the titration. Accurate fitting of the data also requires saturation of the signal. For systems with higher binding affinity, a lower ligand concentration should be used to avoid saturation too early in the titration, which will give inaccurate fits. Once the heat of dilution control (i.e. titration of ligand into buffer) has been subtracted from the titration, the enthalpy at saturation should approach zero. [70].

It is important to know the precise concentration of the sample in the ITC cell and of the ligand in the injection syringe.

A typical analysis with ITC calorimeter is characterized by several stages:

- a) Preparation of the samples (enzyme and ligand in our case)
- b) Setting up the Experiment
- c) Data processing using software provided by the Origin™

## **12.a) Samples preparation**

### *12.a.1) Enzyme preparation*

- The enzyme was dialyzed overnight against buffer to remove glycerol
- After dialysis the enzyme is centrifuged
- The supernatant is diluted in dialysis buffer till 1,85 to 2 ml
- Spectrophotometric measurement at 280 nm of the concentration of the enzyme is done

### 12.a.2 ) *Ligand preparation*

- NADP, NADPH and 6PG were diluted in dialysis buffer
- Measurement of the concentration of the ligand is determined spectrophotometrically

Before to be loaded into the instrument both sample and ligand, are degassed.

### 12.b) **Setting up the Experiment**

- The sample cell is rinsed two or three times with 1.8 ml of distilled water using the proper syringe
- 1.8 ml of macromolecule solution is loaded in the sample cell being careful to avoid bubble formation
- The reference cell is filled with distilled water or buffer.
- The syringe is accurately loaded with the ligand and after removal of any bubble inside, is placed into the sample cell

Parameters for running are set up in the ITC computer (primarily temperature):

- Number of injections = 23
- Injected volume = 10  $\mu$ l
- Time spacing between each injection = 380 seconds
- enzyme concentration = 0,012 mM
- ligand concentration = 0,150 mM for NADPH  
0,5 mM for NADP  
1,74 mM for 6PG

It was made a pre-injection of 5  $\mu$ l and the result from it was not used for data analysis. The different buffers used, with their ionization enthalpy, are reported in Table 8.



<b>Buffer</b>	<b>pK</b>	<b><math>\Delta H</math> (kcal*<math>\text{mol}^{-1}</math>) at 25 °C</b>	<b>Buffer pH range</b>
MES	6,07	3,71	5.5–6.7
MOPS	7,09	5,21	6.5–7.9
HEPES	7,45	5,03	6.8–8.2
TRIS	8,1	11,3	7.5–9.0
TEA	7,8	8,028	7,3-8,3

**Table 8:** pK and  $\Delta H$  ionization of buffers used

### 12.c) Data processing

After correction for dilution enthalpy and for any noise, which was opportunely removed, together with the first point, from the raw thermogram, data were fitted by nonlinear least squares fitting using the software provided by the instrument manufacturer Origin™ (7) to determine:

- the equilibrium constant of association, **K<sub>a</sub>**
- the enthalpy of binding,  **$\Delta H$**
- the stoichiometry of the binding, **n**
- the entropic contribution to the free energy of binding,  **$\Delta S$**

From the initial measurements the Gibbs free energy ( $\Delta G$ ), and entropy change ( $\Delta S$ ) are calculated using the equations:

$$\Delta G = -RT \ln K$$

**Equation 5:** the Gibbs free energy

(in which R is the gas constant and T is the temperature in Kelvin degrees)

$$\Delta G = \Delta H - T\Delta S$$

**Equation 6:** the Gibbs free energy

Since the buffers are able to take or release protons based on their ionization enthalpy, the value of enthalpy calculated by the instrument is corrected taking into account the enthalpy of ionisation of the buffer used. The enthalpy of binding independent from buffer  $\Delta H_0$  [71] was calculated by the equation:

$$\Delta H_{obs} = \Delta H_0 + nH^+ \Delta H_{ion}$$

**Equation 7:** Observed enthalpy equation

( $\Delta H_{obs}$ ).

from which we can obtain the binding enthalpy independent of the buffer ( $\Delta H_0$ )

where  $\Delta H_{ion}$  is the enthalpy of ionisation of the buffer used,  $\Delta H_0$  is the enthalpy measurable in a buffer with  $\Delta H_{ion}=0$ , and  $nH^+$  is the number of hydrogen ions released or captured.

The ionization enthalpy dependence from the temperature is according Fukada and Takahashi [72]

The number of hydrogen ions released or taken is calculated from the equation:

$$nH^+ = \frac{\Delta H_{oss}^1 - \Delta H_{oss}^2}{\Delta H_{ion}^1 - \Delta H_{ion}^2}$$

**Equation 8:** To calculate the number of hydrogen ions released or taken.

where  $\Delta H_{\text{oss}}$  and  $\Delta H_{\text{ion}}$  are the enthalpy of binding observed experimentally and the enthalpy of ionisation of the buffer, respectively.

### 12.c.1) Changes in heat capacity ( $\Delta C_p^\circ$ )

Changes in heat capacity ( $\Delta C_p^\circ$ ) are calculated from the slope value of the linear correlations between the buffer-independent enthalpy change  $\Delta H_o$  for binding and temperature [73].

For the formation of a protein-ligand complex, the  $\Delta C_p$  and  $\Delta H$  can also be calculated from the changes in the polare and apolar solvent exposed surface area ( $\Delta ASA_p$  and  $\Delta ASA_{ap}$ ) [73]. (see equation 9)

$$\Delta C_p = 0.45 \Delta ASA_{ap} - 0.26 \Delta ASA_{pol}$$

**Equation 9:** To calculate changes in heat capacity from exposed surfaces variations (polar / apolar)

$$\Delta H(60) = -8.44 \Delta ASA_{ap} + 31.4 \Delta ASA_{pol}$$

**Equation 10:** reference value obtained at the temperature (60 °C), considered the average denaturing temperature for globular proteins

where  $\Delta ASA$  indicates the variation of accessible surface area.

Knowing the  $\Delta C_p$  and the  $\Delta H$  at any temperature, one obtains a system of two equations with two unknowns values, ( $\Delta ASA_{ap}$  and  $\Delta ASA_{pol}$ ), which can be easily solved.

$\Delta ASA_{ap}$  and  $\Delta ASA_{pol}$  for both the NADP and NADPH binding can also be calculated with the NACCESS program [84], using a probe (sphere) radius of 1.4 Å and a slice width

of 0.1 Å from the structures of sheep liver 6PGDH bound to either a NADP analogue (PDB ID 1PGN) or NADPH (PDB ID 1PGO).

### 12.c.2 ) Effect of pH on dissociation constant

When the binding between the protein and the ligand occurs only in a precise state of ionization, the apparent dissociation constant varies as a function of pH. If only the protonated form of the protein binds the ligand according to the scheme:



decreasing the pH, shifts the equilibrium to the right and the apparent dissociation constant decreases. The intrinsic dissociation constant is then:

$$K_{app} = K_{int} \div \frac{a_{H^+}}{a_{H^+} + 10^{-pKa}}$$

**Equation 11:** The intrinsic dissociation constant.

where  $a_{H^+}$  is the activity of hydrogen ions and is equivalent to  $10^{-pH}$ . In a similar way we proceed if the ligand is present in different states of ionization

### 12.c.3 ) Effect of pH on binding enthalpy

The capture/release of hydrogen ions varies depending on the pH, and is also dependent on the change of the pKa of the ionizable groups in the ligand-protein complex compared to the isolated protein:

$$nH^+ = \sum_i \frac{a_{H^+}}{a_{H^+} + K_i^C} - \sum_i \frac{a_{H^+}}{a_{H^+} + K_i^F}$$

**Equation12:** The capture/release of hydrogen ions depending on the pH and pKa

where  $K_i^C$  and  $K_i^F$  are the  $K_a$  of the ionizable groups in the complex and in the free protein, respectively.

Also

$$nH^+ = \overline{H^C} - \overline{H^F}$$

Where  $\overline{H}$  represents the number of hydrogen ions respectively linked to the complex and the free protein.

$\Delta H_0$  includes the enthalpy changes related to the phenomena of protonation / deprotonation of the protein, and the intrinsic enthalpy of binding  $\Delta H_{int}$  between the ligand and the protein in the correct final state of protonation, will be given by:

$$\Delta H_0 = \Delta H_{int} + \Delta H^C \overline{H^C} - \Delta H^F \overline{H^F}$$

**Equation 13:** enthalpy changes as a function of the protonation / deprotonation and the intrinsic enthalpy binding

where  $\Delta H^C$  and  $\Delta H^F$  are the enthalpies of protonation of the complex and the free protein, respectively.

Can be transformed in

$$\Delta H_0 = \Delta H_{int} + nH^+ \Delta H^F + \partial \Delta H \overline{H^C}$$

**Equation 14:**  $\Delta H_0$  transformed

Where  $\partial \Delta H = \Delta H^C - \Delta H^F$

---

# *RESULTS, DISCUSSION*

## *AND CONCLUSION*

### **Part I. Structural studies. Results and Discussion**

#### **a) Gel-filtration of 6PGDH**

We determined through gel permeation chromatography the molecular weight of the *T. brucei* 6PGDH enzyme, which corresponded to a weight of 104 kDa, the same reported in the literature for the dimeric enzyme. However, when the columns were equilibrated with different ligands, enzyme behavior (in terms of elution volume) varied.

In the presence of NADPH a lower elution volume, corresponding to a molecular weight of ~208 kDa, is observed (Fig. 19A).

In the presence of NADP the elution volume still corresponds to the dimer since no change was observed (Fig. 19A).

In the presence of 6PG, either alone or with NADPH (Fig. 19.B), in both cases the elution volume was in an intermediate position compared to the positions obtained in the presence of NADP and NADPH.

In the presence of both 4PE, an analogue of 6PG thought to mimic a reaction intermediate, and either NADP or NADPH (Fig. 19.C) the elution volume corresponds to a molecular weight of 208 kDa suggesting that the functional ternary complex is a tetramer.

Comparison of the effects of these ligands suggests that the NADPH induces the formation of a tetramer (Fig. 19.A) whereas in the presence of 6PG, either alone or with NADPH, there is a dimer-tetramer equilibration (Fig. 19.B), shown by the intermediate position

between that of the enzyme alone (dimer) and that of the enzyme-NADPH complex (tetramer).

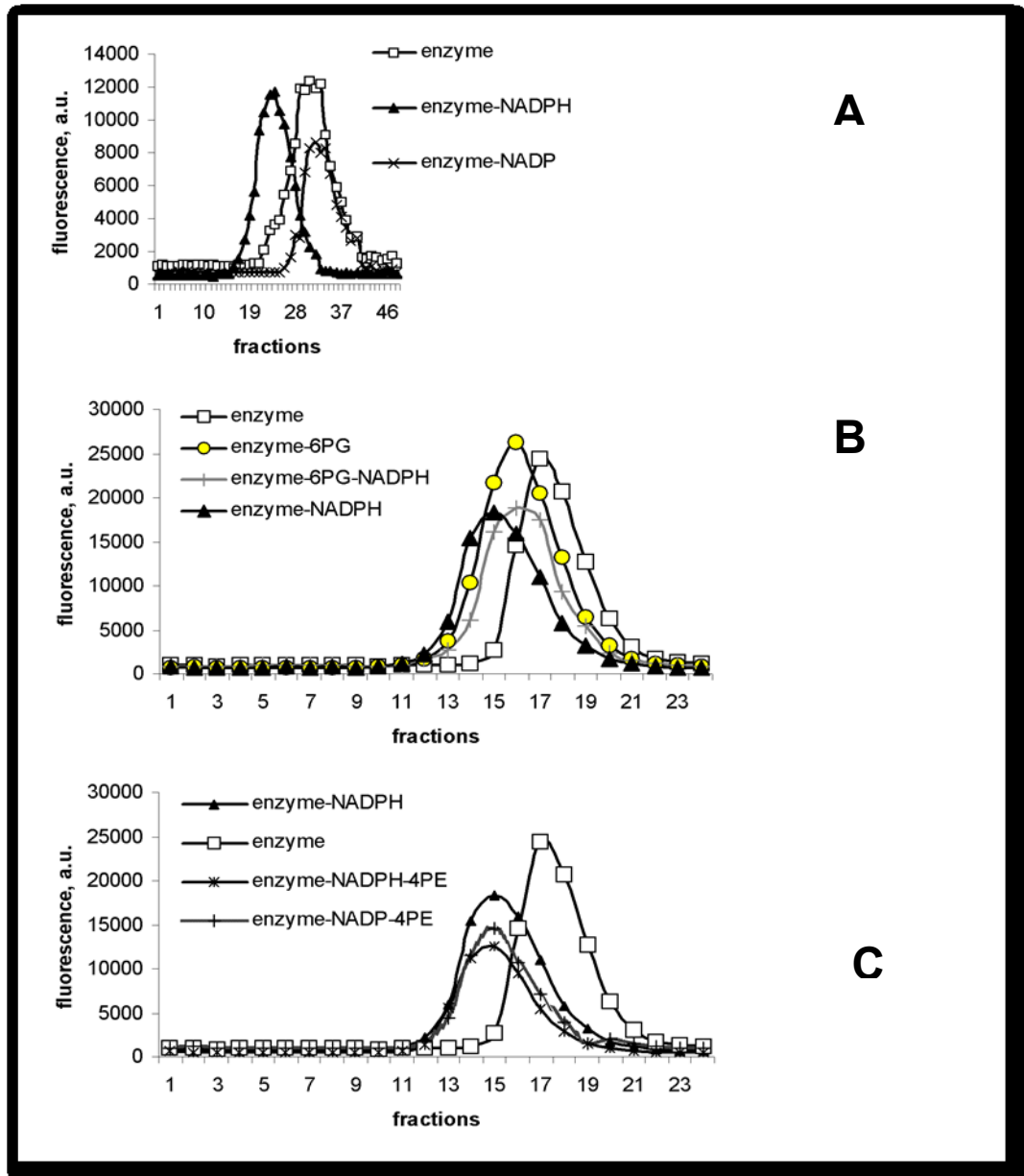


**Figure 19:** Gel-filtration profile of *T. brucei* 6PGDH with and without either NADPH or other ligands. A) From AcA-34, equilibrated with and without each coenzyme. B and C) From Sephacryl S-200. 6PG (the substrate 6-phosphogluconate), 4PE (the dehydrogenation intermediate analogue 4-phosphoerythronate).

The presence of a dimer-tetramer equilibrium induced by ligands in *T. brucei* 6PGDH was further investigated by sucrose density gradient centrifugation, glutaraldehyde cross-

linking, dynamic light scattering and calculation of heat capacity change by microcalorimetry.

## b) Velocity Sedimentation of 6PGDH

Also this technique indicated that NADPH turns out the enzyme to the tetrameric structure, and that in the presence of 6PG the sedimentation behaviour is intermediate between dimer and tetramer (Figure 20). It is noteworthy that the enzyme-NADPH complex sediments as a wide peak, suggesting that a slow re-equilibration tetramer-dimer occurs during the long time of the centrifugation run. This observation is confirmed by the experiments carried out at lower enzyme concentrations, that show a significant shift of the enzyme-NADPH complex toward the dimer (Figure 21).

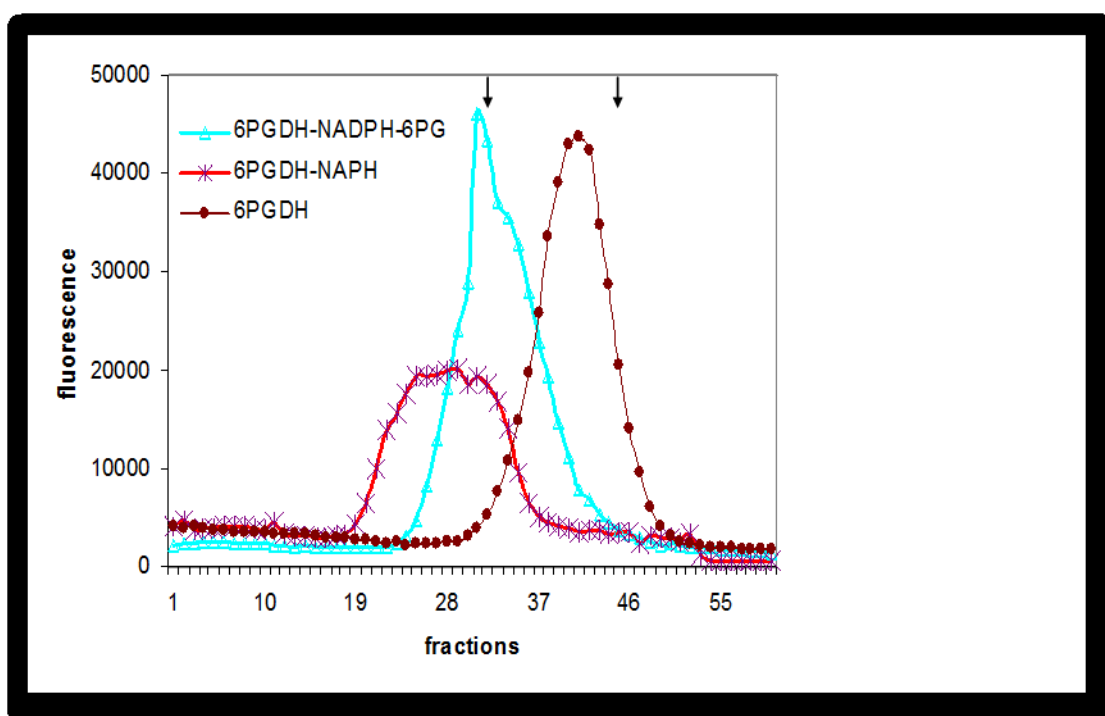


**Figure 20.** Sedimentation of *T. brucei* 6PGDH with and without 0.02 mM NADPH or with both NADPH and 0.16 mM 6PG during sucrose-density gradient centrifugation. Arrowheads show positions of lactate dehydrogenase (140 kDa, the left one) and bovine serum albumin (66 kDa, the right one), used as markers. Protein concentration is around 1 mg/ml.



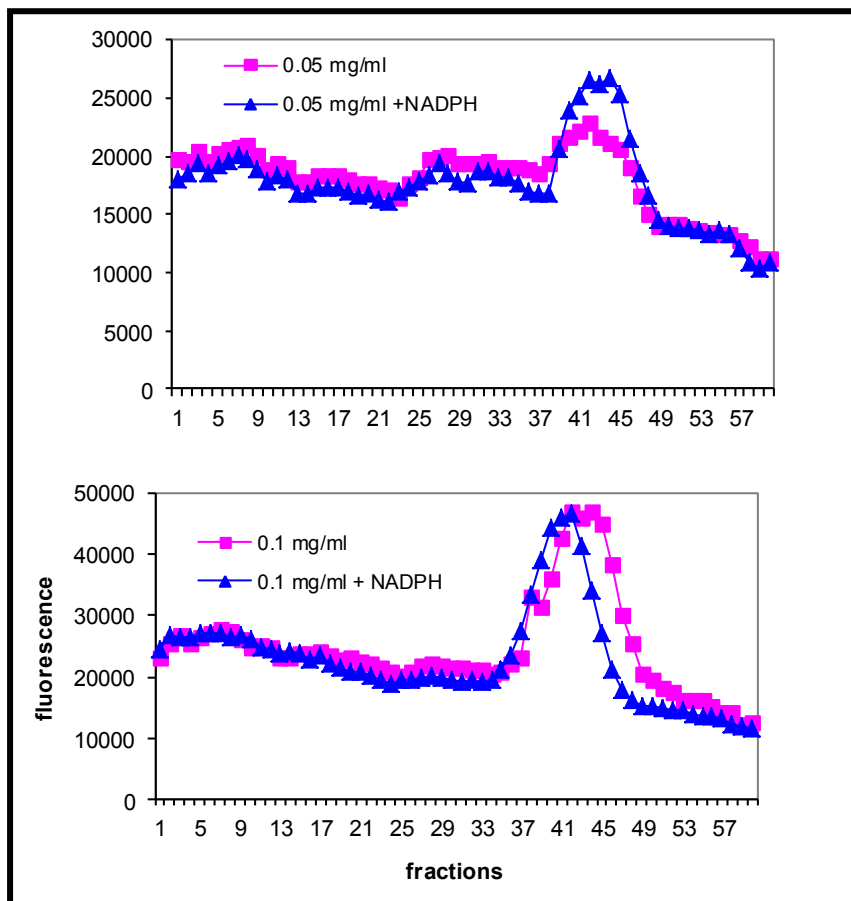


**Figure 21.** Enzyme concentration dependence of the association reaction between dimers to form tetramer for *T. brucei* 6PGDH, in absence or presence of 0.02 mM NADPH.

### c) Glutaraldehyde cross-linking of 6PGDH

We cross-linked the enzyme with glutaraldehyde, either in the presence or in the absence of 40  $\mu$ M NADPH. Surprisingly, we were unable to observe any difference between the enzyme alone and the enzyme-NADPH complex (Fig. 22 A and B). As shown in Figure 22A, both samples show a band at  $\sim$ 100 kDa, the dimer, and two more consistent bands at 200 and 240 kDa. The presence of two bands in the high molecular weight region could be due to a different way of cross-linking, more than to formation of larger aggregates. In fact it is known that proteins containing disulphide bridges in SDS-PAGE show under non reducing conditions a MW larger than under reducing conditions, indicating that the presence of intramolecular cross-linking causes an anomalous migration in SDS-PAGE. In

this case the band at 240 kDa could be caused by the presence of cross-linking within the same subunit.

The lack of a NADPH effect on the cross-linking, and the presence of the high molecular weight species, even with low glutaraldehyde concentrations and short incubation times, both suggest that the equilibrium dimer-tetramer is already present in the enzyme, independently on the ligands presence. In Fig. 22 B also the enzyme not cross-linked is shown, which appears as monomer in these denaturing conditions.

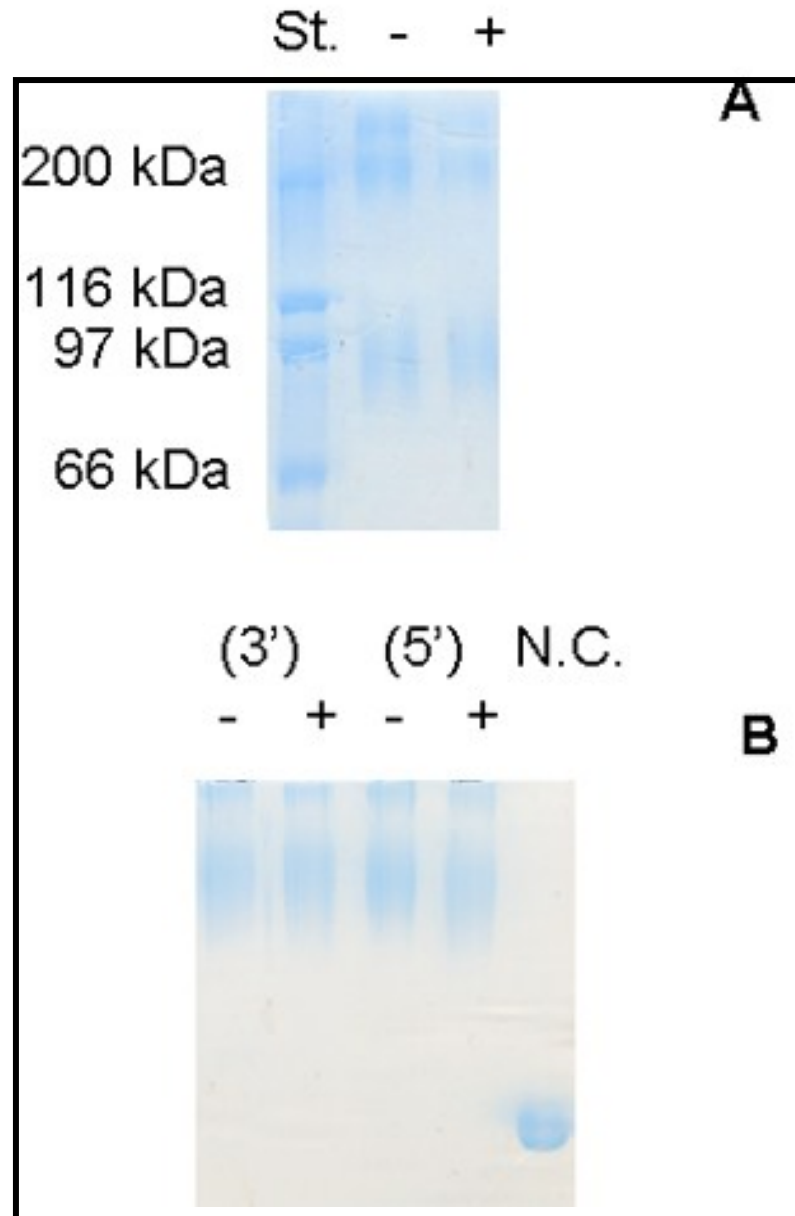


**Figure 22.** (A) SDS-PAGE at 7,5 % acrylamide in the resolving gel, of chemically cross-linked *T. brucei* 6PGDH, in the absence and presence of 40 μM NADPH, incubation with glutaraldehyde was for 1 min. (B) SDS-PAGE at 10 % acrylamide in the resolving gel of chemically cross-linked *T. brucei* 6PGDH, in the absence and presence of 40 μM NADPH, incubation with glutaraldehyde was for 3 and 5 min respectively. St, protein standards, N.C., enzyme not cross-linked with glutaraldehyde (50 kDa).

An other experiment is shown in Fig. 23, where enzyme was treated with glutaraldehyde in absence or presence of both 40  $\mu$ M NADPH and 1 mM 4PE, that is in a condition where the enzyme is in abortive ternary complex. Again it appears that the cross-linking reaction is very fast. Densitometric analysis indicates that the apparent higher proportion of tetramer compared to dimer in the presence of ligands is not significant

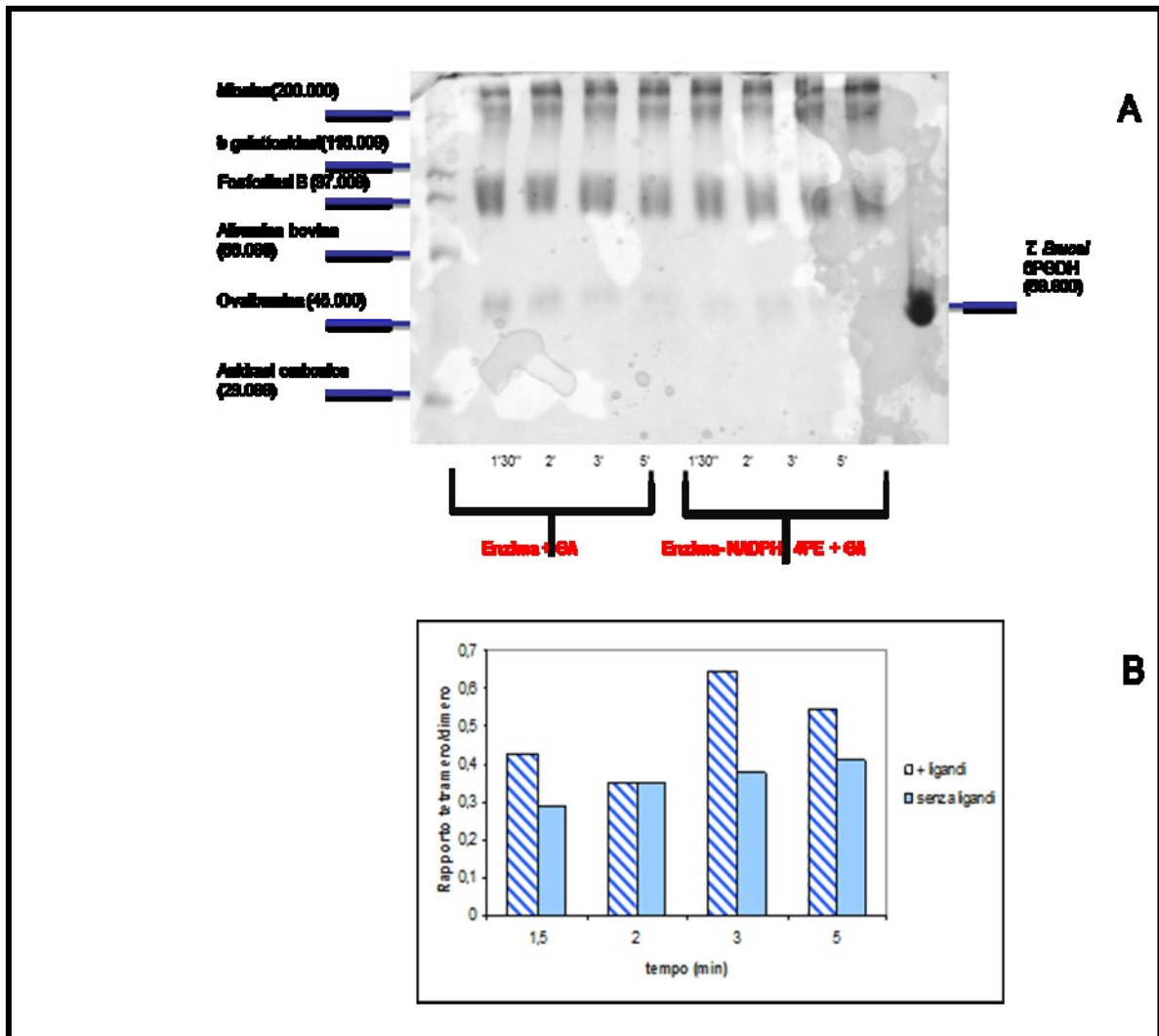


**Figure 23.** (A) SDS-PAGE of *T. brucei* 6PGDH, treated for different times with glutaraldehyde (GA). (B) Densitometric analysis of the tetramer band.

#### d) Dynamic light scattering

The oligomerization of *T. brucei* 6PGDH was studied by DLS. As shown in Table 9, the average hydrodynamic radius of the enzyme increases by increasing the protein concentration, suggesting a concentration dependent association of the protein. However the presence of NADPH, or the presence of both NADPH and 4PE, does not affect the size of the protein. Again the experiments suggest that the dimer-tetramer equilibrium is already present in the enzyme, independently on the ligands presence. A rough calculation of the hydrodynamic radius with HydroPro software (3.94 nm) suggests the presence of larger molecular weight forms even at low protein concentrations.

Sample	T (°C)	Mean R <sup>a</sup> (nm)	St dev
Enzyme 2µM	25	4,739	0,192
Enzyme 2µM + NADPH	25	4,813	0,123
Enzyme 2µM + NADPH + 4-P-Erythronate	25	4,506	0,335
Enzyme 2µM + NADPH + 4-P-Erythronate	5	4,780	0,163
Enzyme 20 µM	25	5,61	0,303
Enzyme 20 µM + NADPH	25	5,521	0,379

**Table 9:** DLS measurements of mean hydrodynamic radius.

<sup>a</sup> R= radius

#### e) ITC- and calculation of heat capacity change

NADP and NADPH have a very different behaviour. In fact the enzyme-NADP complex shows the same behaviour of the free enzyme, suggesting that NADP binding does not modify significantly the rates of oligomerization. To get more information on the differences between NADP and NADPH binding, the binding of the dinucleotides was characterized by ITC. A titration of *T. brucei* 6PGDH with NADP in 50 mM Hepes buffer, pH 7,5 at 15°C is shown in Fig. 24. The K<sub>d</sub> value is 7,54 µM.

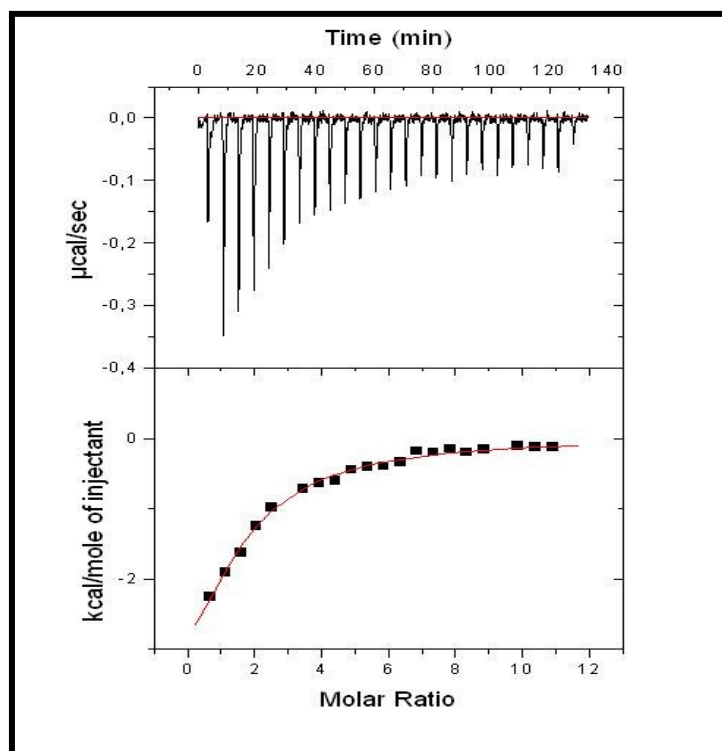


**Figure 24.** *T. brucei* 6PGDH titration with NADP by ITC, in HEPES buffer, pH 7.5 at 15°C.

The experiments were performed at pH 7.5 in different buffers, and the buffer independent binding enthalpy as a function of temperature is reported in Fig. 25. The slopes of the obtained lines give the  $\Delta C_p$  at the binding. There is a remarkable difference between the  $\Delta C_p$  for NADP ( $-92.56 \pm 16,28 \text{ cal/mol}\cdot\text{K}$ ) and that for the NADPH ( $-520,35 \pm 37,44 \text{ cal/mol}\cdot\text{K}$ ). For the formation of a protein-ligand complex, the  $\Delta C_p$  can also be calculated from the changes in the polar and apolar solvent exposed surface area ( $\Delta ASA_p$  and  $\Delta ASA_{ap}$ ) upon the binding [73]. These changes were calculated with NACCESS program from the structures of sheep liver 6PGDH bound to either a NADP analogue or NADPH. While for the NADP binding, experimental and calculated  $\Delta C_p$  are superimposable ( $-92.56$  versus  $-92.63$ ), for the NADPH binding, the experimental value is very different from that calculated ( $-520.35$  versus  $-201.78$ ). There is a decrease of subunit solvent exposed surface at the NADPH binding of ca 2500 Å (Table 10). This suggests that the binding of NADPH to the *T. brucei* 6PGDH causes a conformational change with a large modification of the solvent exposed surface area, much greater than that predicted by the crystal structure in ammonium sulphate, which may be consistent with the existence of a dimer-tetramer equilibrium.

Coenzyme	Experimental $\Delta$ ASA			NACCESS $\Delta$ ASA		
	$\Delta$ ASA <sub>ap</sub>	$\Delta$ ASA <sub>p</sub>	$\Delta$ ASA <sub>tot</sub>	$\Delta$ ASA <sub>ap</sub>	$\Delta$ ASA <sub>p</sub>	$\Delta$ ASA <sub>tot</sub>
NADP	-439	-454	893	-571	-598	-1169
NADPH	-1586	-2063	-3649	-701	-437	-1138

**Table 10:** Comparison between the changes in the subunit polar and apolar solvent exposed surface area ( $\Delta$ ASA<sub>p</sub> and  $\Delta$ ASA<sub>ap</sub> in  $\text{\AA}^2$ ) upon the binding of the coenzymes.

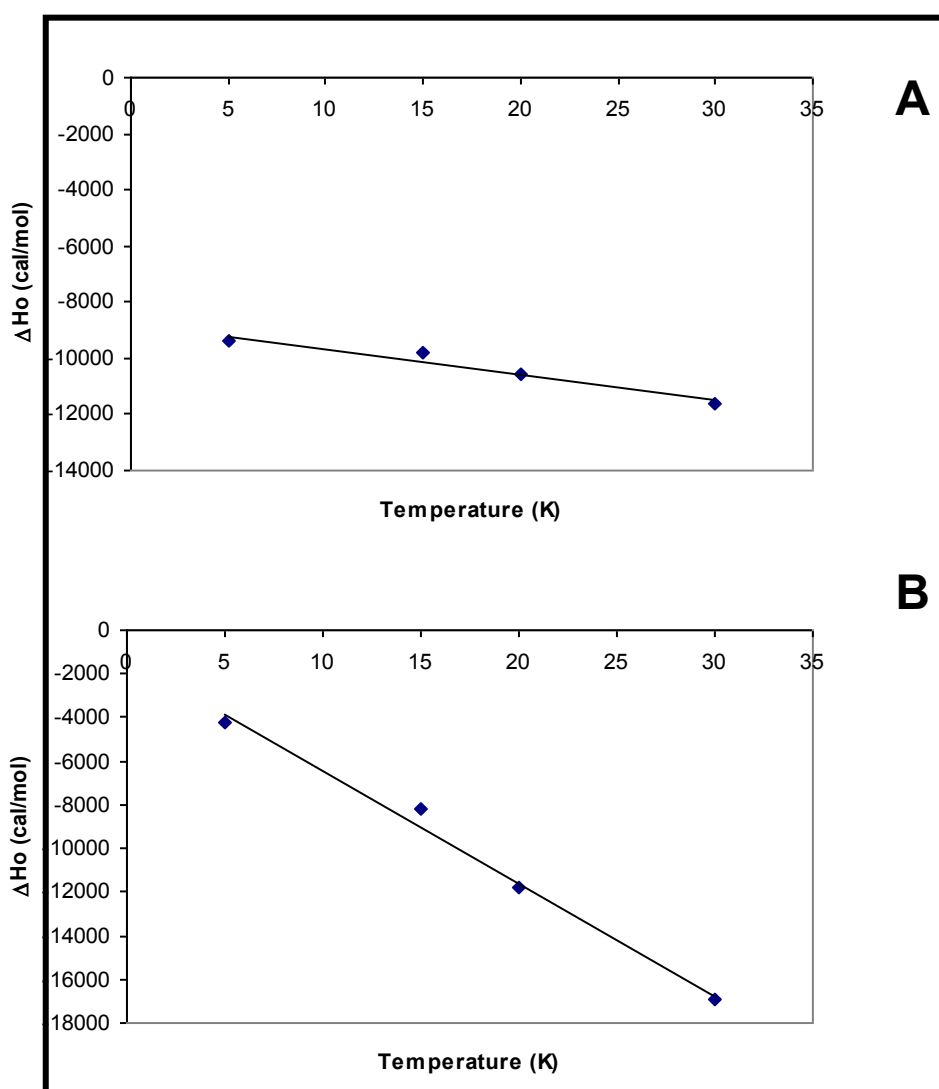


**Figure 25.** Buffer-independent enthalpy change ( $\Delta H_o$ ) dependence from the temperature for the binding to *T. brucei* 6PGDH of NADP (A) and NADPH (B) respectively.

Data till here shown, indicate the presence of a dimer-tetramer equilibrium, but while glutaraldehyde cross-linking and DLS do not suggest any effect of NADPH or of other ligands on this equilibrium, dynamic experiments (gel filtration and sucrose density gradient), where the different oligomeric forms can be separated, show a strong effect of NADPH. We explain these data as a NADPH effect only on the kinetics of oligomerization. In fact if the dimer-tetramer equilibrium in the free enzyme is very fast, in both the gel filtration and density gradient experiments the tetramers dissociate and only dimers are observed. Instead, if the binding of NADPH strongly reduces the rate of association-dissociation of dimers, the tetramers can be observed. If NADPH affects equally the rate of both association and dissociation, the equilibrium dimer-tetramer is not perturbed, therefore DLS and cross-linking are unable to evidence the NADPH effect.

Gel-filtration data indicate that also 6PG reduces the dimers association-dissociation rate, even if less than NADPH, and, more interesting, in the presence of 6PG the reduced coenzyme is no more able to strongly reduce the association-dissociation rate. The antagonism between the substrate 6PG and the coenzyme is a recurrent datum. Examples are the 6PG-induced affinity decrease of the enzyme for NADPH and also the half-site reactivity of 6PGDH for NADP, in the presence of 6PG, or for NADPH, in the presence of 4PE.

To verify whether the ligands effect on the 6PGDH oligomerization is related to other peculiar enzyme properties, we studied in some *T. brucei* 6PGDH mutants, both the NADPH effect on the dimer-tetramer equilibrium rates and the presence of the half-site reactivity at the ternary complex.

#### **f) Dimer-tetramer equilibrium in 6PGDH mutants**

Three site-directed mutants were analyzed: K185R and E192Q, where the mutated residues are involved in catalysis and having very little residual activity, and C372S, with a mutated residue outside from the active site, and a residual enzymatic activity of about 70%. Despite the great differences in enzymatic activity, all the three mutants show, by ITC titration with NADP of the enzyme-4PE complex, a full-site reactivity (almost 2 NADP binding sites/dimer), in contrast to the WT, which presents a full-site reactivity only when the enzyme is not in a binary complex with 4PE (Table 11). Thus, the half-site reactivity displayed by the WT in the ternary complex, in the analyzed mutants is

completely lost, even in the nearly full active C372S. Gel filtration experiments, in the presence and in the absence of NADPH, show that all mutants behave as dimers also in the presence of NADPH (data not shown). Thus the half-site reactivity and the rate of oligomerization share a common mechanism.

<b>Enzyme</b>	<b>K<sub>d</sub> (μM)</b>	<b>Sites/dimer</b>
<b>WT</b>	<b>7.54 ± 0.19</b>	<b>1.86 ± 0.13</b>
<b>WT-4PE</b>	<b>0.043 ± 0.04</b>	<b>1.00 ± 0.003</b>
<b>K185R</b>	<b>5.7 ± 0.1</b>	<b>1.58 ± 0.06</b>
<b>K185R-4PE</b>	<b>1.0 ± 0.05</b>	<b>1.64 ± 0.036</b>
<b>E192Q</b>	<b>2.0 ± 0.09</b>	<b>1.72 ± 0.05</b>
<b>E192Q-4PE</b>	<b>0.138 ± 0.035</b>	<b>1.51 ± 0.07</b>
<b>C372S</b>	<b>4.5 ± 0.8</b>	<b>1.74 ± 0.11</b>
<b>C372S-4PE</b>	<b>0.02 ± 0.017</b>	<b>2.02 ± 0.26</b>

**Table 11:** Binding parameters of NADP to 6PGDH from *Trypanosoma brucei*, in Hepes buffer, pH 7.5, at 20°C.

## **Part I. Structural studies. Conclusion**

The physiological significance of the dimer-tetramer equilibrium, and of the effects of NADPH and 6PG, is unclear. 6PG has several effects on the 6PGDH: not only it decreases the NADPH inhibition by increasing the K<sub>d</sub>/K<sub>i</sub> [19,75,76], but also it induces the half-site reactivity for NADP [19,37], acts as allosteric activator [74], and promotes the decarboxylation of the 3-keto intermediate [38]. Furthermore NADPH is not simply an inhibitor and a product of the reaction. In fact it promotes the conversion of Ru5P to the enolate intermediate in the reverse reaction [77,78], and again promotes the decarboxylation of the 3-keto intermediate [38,79]. In the present report we find another property of 6PG and NADPH, the effect on the rate of dimer-tetramer equilibrium of the enzyme.



However the intracellular concentration of 6PGDH is usually low enough to keep the enzyme in the dimeric form, providing that the low water activity of the cytosol does not alter the equilibrium. Nevertheless we cannot ignore the very attractive hypothesis, that the experimental evidences here reported are related to the regulation of the 6PGDH activity.

An indirect evidence that the effect on the association-dissociation rate is related to other peculiar properties of the enzyme comes from the behaviour of the enzyme mutants. Both the nearly inactive enzymes (K185R and E192Q) and the nearly full active enzyme (C372S) display neither the effect of NADPH on the oligomerization rates nor the half-site reactivity in the ternary complex. This means that perturbations of the conformational changes affecting the rate of oligomerization also affect the correct formation of the ternary complex.

The pentose phosphate pathway is regulated by the NADPH/NADP ratio that inhibits/activate the glucose-6-phosphate dehydrogenase (G6PD) leading to the formation of 6PG. Also the 6-phosphogluconate dehydrogenase is strongly inhibited by NADPH, and its maximal activity in *T. brucei* is nearly equal to the activity of G6PD [80]. It has been reported that in cancer cells, where the glycolysis is strongly enhanced, depletion of G6PD affects the cell viability only under oxidative stress [81], while depletion of 6PGDH and accumulation of 6PG, affect the cell viability also in the absence of oxidative stress [82]. In *T. brucei* bloodstream form, where the glycolysis is the only energy source, it is mandatory to ensure an efficient clearing of the 6PG [78]. All the previously reported 6PG effects promote an increased catalytic efficiency of the enzyme, and the present observation of the 6PG effect on the enzyme association/dissociation rate suggests that, also in the present case, we deal with a yet unclear mechanism to surmount the NADPH inhibition.

---

# RESULTS, DISCUSSION

## AND CONCLUSION

### Part II. Functional studies. Results and Discussion

The pH dependence of  $V$  and  $V/K$  for the *T. brucei* 6PGDH, have been already determined [85] Both  $V$  and  $V/K$  show a bell-shaped curve. Also the  $pK_m$  for 6PG and NADP against pH have a bell shape. As shown in Figure 26, two  $pK_a$ , 7.17 and 9.65, can be observed in the graph with  $pK_m$  for 6PG. The group with  $pK_a$  7.17 is likely one of the groups that release  $H^+$  upon binding of 6PG, always it has been thought the lysine 185  $pK_a$ , that must be non-protonated in the enzyme substrate complex while the  $pK_a$  9.65 is likely that of the glutamate 192 in the enzyme-substrate complex, that must be protonated in the enzyme substrate complex.

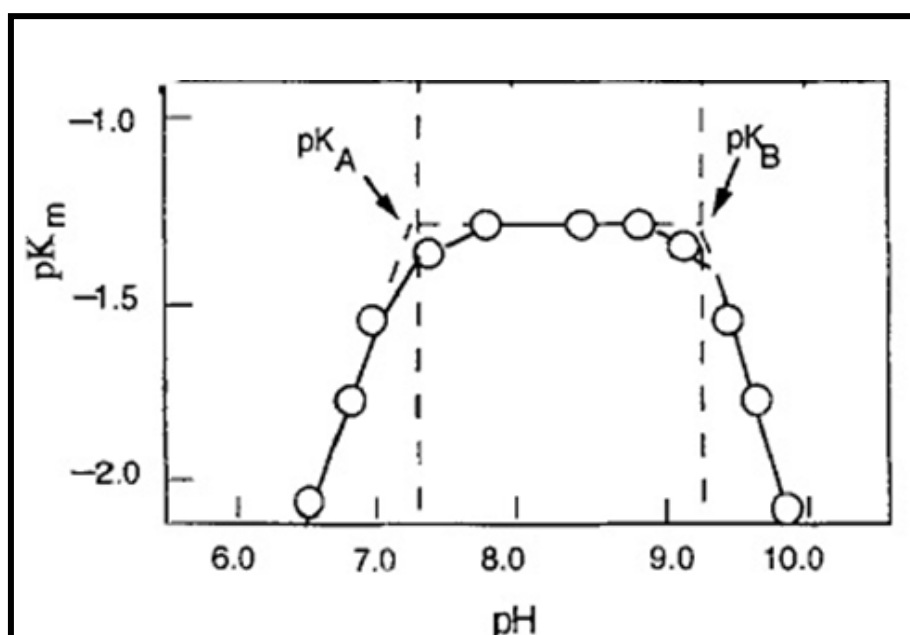


Figure 26:  $pK_m$  dependence from pH for 6PG in *T. brucei* 6PGDH [85]

## a) Effect of mutation on the enzyme activity

### a.1) E192Q

This mutant show a strongly decreased enzymatic activity, the specific activity is  $0.028 \mu\text{mol min}^{-1}\text{mg}^{-1}$ , against a value of  $20 \mu\text{mol min}^{-1}\text{mg}^{-1}$  for the WT. The pH dependence of  $V_{\text{max}}$  is, within the experimental error, a flat line similar to that observed in the E190Q mutant of the sheep liver enzyme. [28]

### a.2) K185H

This mutant presents a peculiar biphasic kinetics, with an initial faster phase producing few equivalents of product, followed by a second slow, steady state phase. The rate of the fast phase is about three orders of magnitude lower than WT ( $0.013 \mu\text{mol min}^{-1}\text{mg}^{-1}$ ), while the rate of the steady-state phase is four orders of magnitude lower than WT (Figure 27). The specific activity value for the initial phase is approximate, due to the non-linear kinetics, and other classical kinetic parameters could not be determined, for the same reason. Analysis of the burst kinetics shows that the initial rate is approximately proportional to the enzyme concentrations, and its amplitude depends on the concentrations of the substrates. The rate of the slow phase loses dependence on the enzyme concentration, but it depends only from the amplitude of the fast phase. This suggests that during the fast phase there is an approach to the equilibrium of the enzyme-catalyzed reaction, with the formation of an unknown intermediate. This intermediate decays non-enzymatically during the slow phase, causing a further progress of the enzymatic reaction. The burst-phase amplitude, extrapolated to time zero, measured at different concentrations of the substrates and at different pH, allowed the equilibrium constant between reagents and products to be calculated. The calculated value, taking into account the hydrogen ion concentration, was  $6.3 \cdot 10^{-12}$  M, close to  $1.84 \cdot 10^{-11}$  M, the  $K_{\text{eq}}$  for the dehydrogenation of 2-deoxy 6-phosphogluconate to 3-keto 6-phosphogluconate [30] suggesting that the intermediate is the 3-keto 6-phosphogluconate. The low amount and the low stability of the intermediate precluded an unambiguous identification.

Despite the reaction product has not been identified, the reaction seem to be arrested after the dehydrogenation. In the next step, the decarboxylation of the 3-keto-6-phosphogluconate, lysine 185 should give an  $H^+$  to the 3-keto oxygen to give the dienol intermediate. The  $pK_a$  of the histidine should be too low to be protonated, thus the decarboxylation is impaired. At the same time while the protonated lysine contributes to the strong binding of the keto intermediate, the non-protonated histidine could allow the release of the 3-keto-6-phosphogluconate in the medium.

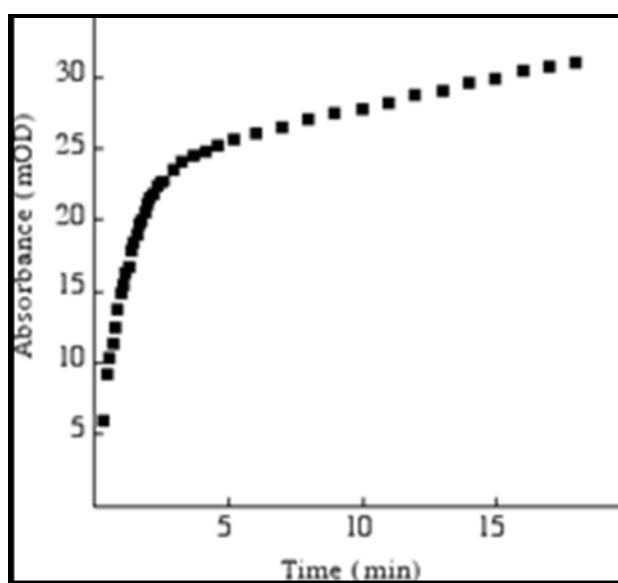


Figure. 27: Kinetics of the mutant K185H.

### a.3) H188L

This mutant shows only a moderate decrease of the enzymatic activity ( $1.31 \mu\text{mol min}^{-1} \text{mg}^{-1}$  against 20 for the WT). The  $V/K_{\text{NADP}}$  is pH dependent showing two  $pK_a$ , 6.95 and 9.6, very close to the  $pK_a$  observed for the WT enzyme (not shown).

### b) Cysteine reactivity

Not only kinetic studies show that 6PG binding potently effects the enzyme [74] but also structural studies like reactivity toward chemicals, denaturing agents and proteolysis evidence that in the presence of the substrate there is a strong reactivity reduction, consistent with an induced conformational change of the enzyme [31]. DTNB titration

allows to measure cysteine reactivity, in the *T. brucei* WT three cysteines for subunit are fast titrated at pH 7.5, but in presence of 6PG one cysteine alone is titrated in more than 10 minutes (Figure. 28). Also in the mutant E192Q and K185H there is a reduction of reactivity in the presence of 6PG (data not shown). Instead in the H188L mutant the cysteine reactivity is still high also in the presence of 6PG (Figure 28).

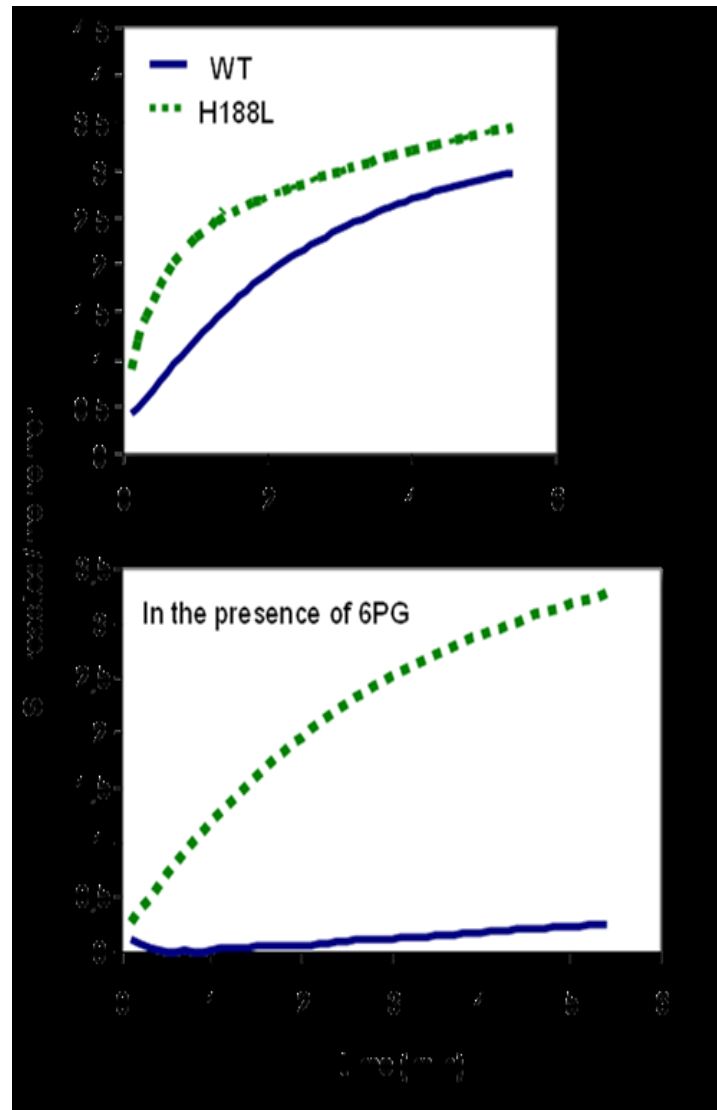


**Figure 28:** The cysteines reactivity in absence and in presence of 6PG for WT and H188L mutant.

**c) 6PG binding to 6PGDH**

The binding of 6PG to 6PGDH has been studied by ITC in the WT enzyme and in three mutants: E192Q, K185H and H188L. While E192 and K185 are the active site residues involved in catalysis, H188 is a conserved residue at 4-5 Å from E192.

The proton uptake/release accompanying the binding has been measured at three different pH, titrating the enzyme in different buffers. The data are summarized in Table 12.

<u>Enzyme</u>	<u>K<sub>d</sub> (M)</u>	<u>pK<sub>a</sub></u>	<u>nH<sup>+</sup></u>		
			<b>pH 6.5</b>	<b>pH 7.5</b>	<b>pH 8.5</b>
<u>Wt</u>	2.5 10 <sup>-6</sup>	7.54	-0.346*	-0.463	-0.695
E192Q	3.12 10 <sup>-5</sup>	<u>nd</u>	-0.234	-0.889	-1.809
K185H	1.39 10 <sup>-6</sup>	7.45	-0.308	0.469	0.408
H188L	2.71 10 <sup>-5</sup>	7.2	-0.302	-0.451	-0.18

**Table 12:** Intrinsic  $K_d$ ,  $pK_a$  and number of proton exchanged at the 6PG binding.

\*The sign – indicates proton release, values refer to enzyme subunit, nd, not detected.

*c.1) The binding of 6PG to 6PGDH WT*

The binding of 6PG to 6PGDH shows a pH dependence indicating the requirement of a protonated group with  $pK_a$  7.07 (Figure 29). On the basis of the observed  $K_d$ , no proton release is expected, while a proton uptake is expected at pH higher than 7.0. Instead at all pH tested the binding is accompanied by a release of hydrogen ions. The  $pK_a$  of 6PG is 6.3 [83] therefore if only the ionized form of the substrate binds to the enzyme, at pH 6.5 the proton release can be totally accounted for by the ionization of 6PG. The  $pK_a$  decrease at pH lower than 7 suggests that unprotonated 6PG binds to the enzyme. However at pH >7.0, other group(s) must be involved to balance the observed protons release. At least 1.5  $H^+$  are required to account for the proton uptake of the group with  $pK_a$  7.07 and the release of  $H^+$  observed experimentally. A scheme with three residues involved is shown in Figure

30, where that with the pK of 7.07 binding a proton released by a second residue, while a third residue releases hydrogen ions in the buffer.

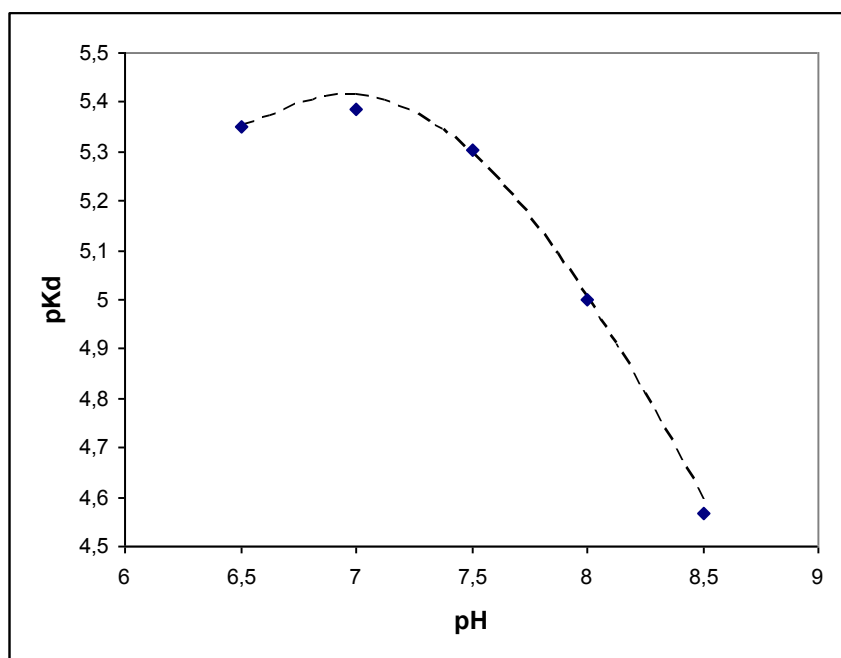


Figure 29: pH dependence for 6PG apparent  $pK_d$

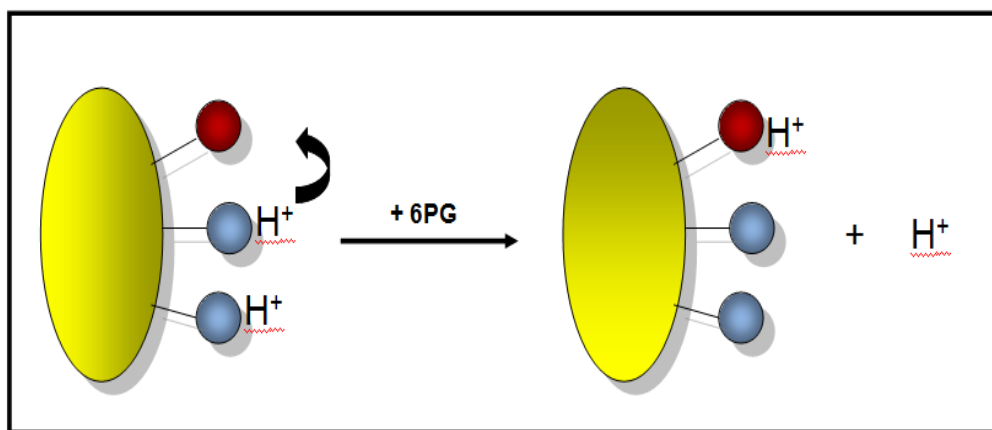


Figure 30: Scheme with three residues involved in the change of the protonation state of the enzyme at the substrate binding

*c.2) The binding of 6PG to E192Q mutant*

This mutant shows a  $K_d$  pH independent (data not shown), and one order of magnitude higher than that of the WT enzyme. This suggests that the group with  $pK_a$  7.07 observed in the WT enzyme is absent in the mutant. Accordingly to the proposed mechanism of 6PGDH, the glutamate 192 should become protonated in the enzyme-substrate complex. We measured the proton uptake/release of the E192Q mutant, where the mutated residue cannot accept  $H^+$ . At pH 6.5 the behaviour of the mutant is identical (within the experimental error) to the WT. However at higher pH the binding is accompanied by a large proton release, reaching about 1.8  $H^+$  released at pH 8.5. The excess of proton release, i.e the difference between WT and E192Q enzymes, is coherent with the lack of a protonable group with  $pK_a$  7.0. The data evidence the lack of a proton-accepting group, and suggest that the group that must be protonated for the binding of 6PG is E192.

The 6PG binding enthalpy increase, at higher pH correlates with augmentation in the number of  $H^+$  released (Table 13). As already shown 6PG binding is mainly entropy driven, with entropy gain resulting from the desolvation of the phosphate [19].

pH	$\Delta H_o$ (cal/mol)	$nH^+$
6,5	-633	-0,234
7,5	2992	-0,889
8,5	4760	-1,809

**Table 13:** Buffer-independent enthalpy change and number of hydrogen ions exchanged at different pH in the mutant E192Q at the 6PG binding.



### *c.3) The binding of 6PG to K185H mutant*

Lysine 185 is thought the residue that accepts the hydrogen ion from the 3 OH of the 6PG during the first step of the catalysis and should be non protonated in the enzyme substrate complex. Thus this residue is expected to be one of the two groups that release  $H^+$  upon substrate binding. The  $K_d$  of the K185H mutant is pH dependent with an apparent  $pK_a$  of 7.4 (table 12), meaning that the group that must be protonated in the enzyme-substrate complex is still present. Mutation of K with H, whose natural  $pK_a$  is about 3.5 units lower than the  $pK_a$  of the lysine, should cause the disappearance of an hydrogen donating group from the proton balance. In fact the mutant K185H shows, at pH 7.5 and 8.5, an uptake of  $H^+$ , while at pH 6.5, where also the histidine is protonated, the mutant behaves like the WT. The difference in proton balance between WT and K185H enzymes, is coherent with the lack of a  $H^+$  releasing group with  $pK_a$  7.4. The data suggest that 6PG binds to the protonated form of the enzyme (into both the residues K185 and E192) and, upon binding, K185 releases its hydrogen ion.

### *c.4) The binding of 6PG to H188L mutant*

H188 is conserved in all the 6PGDHs and is buried at 4-5 Å from E192. This residue was mutated to L, to keep a bulky side chain. The  $K_d$  of the H188L is one order of magnitude higher than that of the WT enzyme, and it is pH dependent with an apparent  $pK_a$  of 7.2, meaning that the group that must be protonated to bind the substrate is still present. The proton release was very similar to the WT enzyme with only pH 8.5 showing significant differences. From the number of proton exchanged upon the binding it is possible to recover a change in  $pK_a$  of the residues involved (see methods). The difference in proton release between WT and H188L suggests that the mutant enzyme lacks of a group whose  $pK_a$  drops from >10.0 to 8.65 upon binding of the substrate. These  $pK_a$  are hardly attributed to a buried histidine, and probably reflect small conformational changes accompanying the binding of the substrate.

The current mechanism hypothesized for 6PGDH requires that two essential groups, K185 and E192, invert its ionization state upon binding of the substrate, K185 becoming

unprotonated while E192 protonated. Our results give experimental support to the proposed mechanism, in fact the lack of the proton-accepting group, E192, causes a greater  $H^+$  release, while the lack of the proton releasing group, K185, causes an  $H^+$  uptake. Starting from these observations it is possible to describe the ionization state of the free and substrate bound enzyme.

6PGDH has a rapid equilibrium random kinetic mechanism [86], and with 6PG maintained at a saturating concentration, the kinetic mechanism can be described schematically as shown in Figure 31.

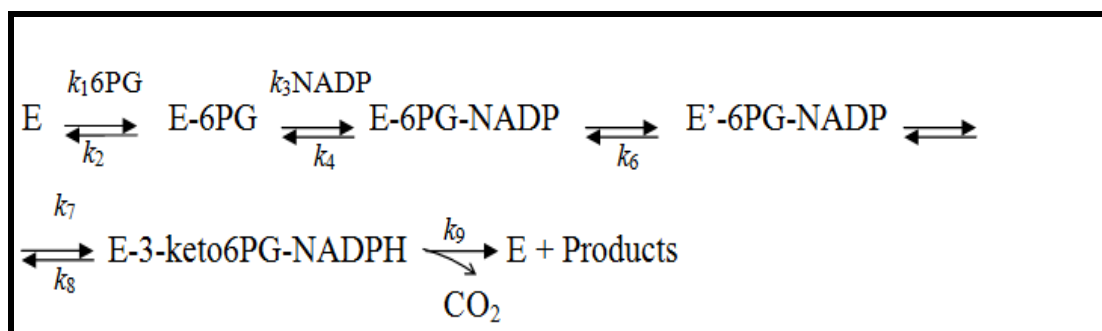


**Figure 31:** Kinetic mechanism of 6PGDH

The  $pK_a$  of the two residues in the enzyme-substrate complex can be obtained by the pH dependence of  $V/K_{NADP}$ . In fact  $V/K$  is

$$\frac{V}{K} = \frac{k_1}{1 + \frac{k_2}{k_3} \left( 1 + \frac{k_4}{k_5} \left( 1 + \frac{k_6}{k_7} \left( 1 + \frac{k_8}{k_9} \right) \right) \right)}$$

**Equation 15.** V/K equation

In this equation  $k_i$  and  $k_{i+1}$  refer to the conversion of the same intermediate specie in the forward and reverse directions, and this, accordingly to the mechanism (Figure 31 and equation 15), requires the same ionization state for the catalytic residues involved in the reaction. Thus a change in the ionization of catalytic residues induced by pH should affect at the same extent both rate constants. The only rate that can be still dependent on the pH is  $[E]k_1$ , where  $[E]$  is the fraction of correctly protonated enzyme, i.e. the fraction of

catalytically competent enzyme. In the case of  $V/K_{\text{NADP}}$  the catalytically competent enzyme is the enzyme-6PG complex, and shows two  $pK_a$ , 7.17 and 9.65. The  $pK_a$  7.17 could be assigned to the K185, that must be non-protonated in the enzyme substrate complex, while the  $pK_a$  9.67 could be assigned to the E192, that must be protonated in the enzyme substrate complex.

In the free enzyme the pH dependence of the dissociation constant of *T. brucei* 6PGDH for 6PG evidences the requirement of a protonated group with  $pK_a$  7.07. Despite this  $pK_a$  appears anomalous for a glutamate, it can be assigned to the glutamate192, in fact mutation of this residue with glutamine causes the disappearance of the pH dependence of the  $K_d$ . Furthermore the difference in  $H^+$  release between WT and E192Q mutant enzymes fit fairly well with the disappearance of a group whose  $pK_a$  changes from 7.07 to 9.67, upon substrate binding. The requirement of a protonated form for the glutamate 192 can be easily predicted by its proximity with the carboxylate group of the substrate. The crystal structure of 6PGD-6PG complex is available for the enzymes from sheep liver (1PGD), *E. coli* (2ZYA) and *Geobacillus stearothermophilus* (2w8z). Despite small differences in substrate conformations, the glutamate is in all cases less than 4.0 Å from the carboxylate of 6PG.

The  $pK_a$  of K185 in the free enzyme can be evaluated from the proton uptake of the K185H mutant. In fact the differences in  $H^+$  release/uptake between WT and K185H mutant enzymes should correspond to the  $H^+$  released by K185. The data are consistent with a group changing its  $pK_a$  from 9.3 to 7.17, therefore a  $pK_a$  9.3 can be estimated for K185 in the free enzyme.

At pH 6.5 and pH 8.5, the proton balance evidences that other residues are involved in the binding. At pH 6.5 the excess of  $H^+$  can be assigned to the dissociation of 6PG, in fact both WT and mutant enzymes show a very similar proton release that corresponds to the ionization of 6PG ( $pK_a$  6.3). At pH 8.5 it is likely that the excess of  $H^+$  release does not arise from a single group, but is the result of several small ionization changes induced by the conformational changes accompanying the substrate binding. Nevertheless all these

changes can be collectively described with good approximation by a single group. Thus a minimal model for the ionization changes induced by the substrate binding should account for three groups: the glutamate 192, whose  $pK_a$  increases from 7.07 to 9.67, the lysine 185 whose  $pK_a$  decreases from 9.3 to 7.17, and a third group whose  $pK_a$  is downshifted.

The differences in  $H^+$  release between WT and H188L mutant enzymes can be described with a group changing its  $pK_a$  from 10.5 to 8.65. These  $pK_a$  values are hardly attributable to the histidine 188, instead it is likely that arise from different small ionization changes due to the conformational changes induced by the substrate. In fact the more interesting property of this mutant is the absence of the effect of 6PG on the reactivity of thiol groups. In the wt enzyme the binding of 6PG suppress the reactivity of all cysteine residues, and this can be explained only by a conformational effect. K185H and E192Q mutants show, with few differences, the same 6PG effect on the reactivity of the cysteine residues, but in the H188L mutant the presence of 6PG does not change significantly the reactivity of cysteine residues. For this reason we suggest that the differences in  $H^+$  release between WT and H188L mutant are due to the conformational changes induced by substrate, and that all ionization changes can be collectively described as a single group changing its  $pK_a$ .

In conclusion the  $H^+$  release/uptake of 6PGDH WT and its mutants can be described with good approximation taking into account three enzyme groups and 6PG (Figure 32): lysine 185 (lacking in the K185H mutant) with  $pK_a$  changing from 9.3 to 7.17; glutamate 192 (lacking in the E192Q mutant) with  $pK_a$  changing from 7.07 to 9.67; a group representing at least part of the conformational changes (lacking in the H188L mutant) with  $pK_a$  changing from 10.5 to 8.65; 6PG with  $pK_a$  6.3 that binds only in the ionized form.

With a reasonable model available for the ionization changes occurring with the formation of the enzyme-substrate complex, it is also possible to assign the ionization enthalpies to the single residues by comparing the binding enthalpies of the 6PG to the WT enzyme with the binding enthalpies of the mutants.

The difference in the binding enthalpy between WT and E192Q mutant, together with the difference in proton release, gives the enthalpy contribution of the protonation of the glutamate 192. In the same way the difference in the binding enthalpy between WT and K185H mutant gives the contribution of the protonation of the lysine 185 and the difference in the binding enthalpy between WT and H188L mutant gives the contribution of the protonation changes attributed to the conformational changes. With the only exception of E192Q at pH 8.5, the data at different pH fits quite well giving for the E192 a  $\Delta H -3.5 \pm 0.9$  kcal/mole, for K185  $\Delta H -9.83 \pm 1.6$  kcal/mole, and for conformational changes  $\Delta H 7.97 \pm 0.95$  kcal/mole. From these values, and from the model for the change in the ionization state previously described, the intrinsic binding enthalpy can be calculated, i.e. the binding enthalpy for the correctly protonated substrate to the correctly protonated enzyme. The calculated intrinsic binding enthalpy is  $-4.6 \pm 0.23$  kcal/mole, and this value, although it includes both experimental and fitting errors, clearly shows that a large part of the binding enthalpy is spent to put the enzyme in the correct protonation form. Accordingly to the proposed mechanism (Figure 31) at the end of the reaction the protonation of the enzyme-product complex is the same of that of the free enzyme, therefore the energy spent during the binding of the substrate will be regained during the catalytic cycle.

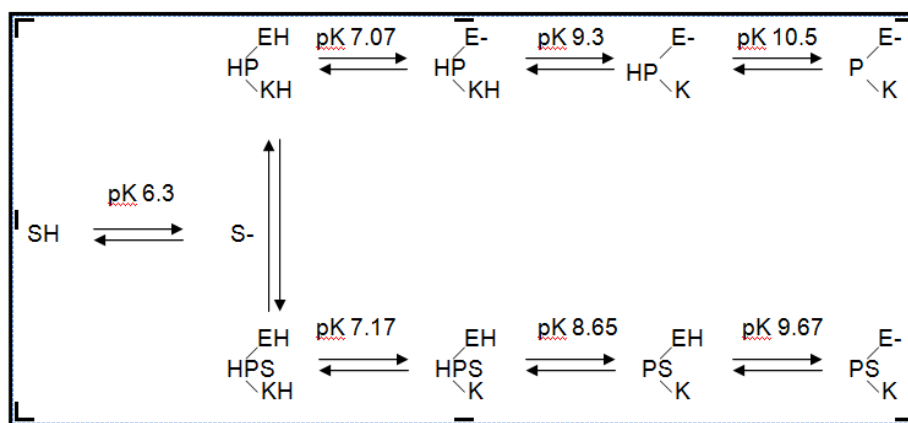


**Figure 32:** Scheme for the  $pK_a$  shifts for ionizable residues in the *T. brucei* 6PGDH upon formation of the enzyme-6PG complex. S, substrate 6PG, P, enzyme, E, E192, K, K185.

## **Part II. Functional studies. Conclusion**

The model described, even if simplified, allows to describe with good approximation, the change in the protonation state of 6PGDH upon substrate binding.

The main uncertainty comes from the operative need to put in one  $pK_a$  change the ionization variations due to conformational changes, while most probably a number of groups are involved.

Data show that K185 is unprotonated in the enzyme-substrate complex while E192 is protonated. Furthermore in the bell  $K_{6PG}$ -pH curve the two pK of 7 and 9.5 have always been attributed to K185 and E192 but being so different from the natural pK of a lysine and glutamate it was thought that they were only apparent pK and only a small fraction of the enzyme was in the right protonation state, able to display the catalytic activity. Our results show that the pK of K185 and E192 really can move after the substrate binding to the values of 7 and 9.5, respectively. Thus kinetic parameters with good approximation correspond to the true pK of key aminoacids in catalysis.

---

## REFERENCES

- [1] Prashant P., Joshi; herder, Stephane; Truc, Philippe. **Human Trypanosomiasis caused by *Trypanosoma evansi* in India: The first case report.** *J Trop. Med* 2005 73 (3). pp 491-495.
- [2] Barrett, M. P. **The fall and rise of sleeping sickness.** (1999). *The Lancet* , 353, 1113-4.
- [3] Cavalier-Smith, T. **Kingdoms Protozoa and Chromista and the eozoan root of the eukaryotic tree.** (2010). *Biology Letters* 6, 342–345
- [4] Paul T. Manna, Steven Kelly, Mark C. Field. **Adaptin evolution in kinetoplastids and emergence of the variant surface glycoprotein coat in African trypanosomatids.** (2013). *Molecular Phylogenetics and Evolution*. 67 pp 123–128
- [5] Natalie A. Stephens and Stephen L. Hajduk. **Endosomal Localization of the Serum Resistance-Associated Protein in African Trypanosomes Confers Human Infectivity.** (2011) *Eucaryotic cell*. p. 1023–1033.
- [6] Ripamonti D, Massari M, Arici C et al. **African Sleeping Sickness in Tourists Returning from Tanzania: The First 2 Italian Cases from a Small Outbreak among European Travelers.** (2002) *Clin Infect Dis*. (34):e18-e22
- [7] Gautret P, Clerinx J, Caumes E et al. **Imported human african trypanosomiasis in Europe, 2005-2009.** (2009). *Euro Surveill*.14(36):p 19327
- [8] Programme Against African Trypanosomosis. **Tsetse and Trypanosomiasis information** (2011) (35) p 12
- [9] Margaret A. Phillips. **Stoking the drug target pipeline for human African trypanosomiasis.** (2012) *Molecular Microbiology*. 86(1), 10–14
- [10] Barrett, M.P., Boykin, D.W., Brun, R., and Tidwell, R.R. **Human African trypanosomiasis: pharmacological reengagement with a neglected disease .** (2007). *Br J Pharmacol* 152: 1155–1171.
- [11] Morgan, H.P., McNae, I.W., Nowicki, M.W., Zhong, W., Michels, P.A., Auld, D.S., et al. **The trypanocidal drug suramin and other trypan blue mimetics are inhibitors of pyruvate kinases and bind to the adenosine site.** (2011) *J Biol Chem* 286: 31232–31240.
- [12] Jacobs, R.T., Nare, B., and Phillips, M.A. **State of the art in African trypanosome drug discovery.** (2011.a). *Curr Top Med Chem* 11: 1255–1274.

- [13] Wilkinson, S.R., Taylor, M.C., Horn, D., Kelly, J.M., and Cheeseman, I. **A mechanism for cross-resistance to nifurtimox and benznidazole in trypanosomes.** (2008). *Proc Natl Acad Sci USA* **105**: 5022–5027.
- [14] Lanteri, C.A., Tidwell, R.R., and Meshnick, S.R. **The mitochondrion is a site of trypanocidal action of the aromatic diamidine DB75 in bloodstream forms of *Trypanosoma brucei*.** (2008) *Antimicrob Agents Chemother* **52**: 875–882.
- [15] Alsford, S., Eckert, S., Baker, N., Glover, L., Sanchez-Flores, A., Leung, K.F., *et al.* **High-throughput decoding of antitrypanosomal drug efficacy and resistance.** (2012) *Nature* **482**: 232–236.
- [16] Hall, B.S., Bot, C., and Wilkinson, S.R. **Nifurtimox activation by trypanosomal type I nitroreductases generates cytotoxic nitrile metabolites.** (2011) . *J Biol Chem* **286**: 13088–13095.
- [17] Aronov, A. M.; Suresh, S.; Buckner, F. S.; Van Voorhis, W. C.; Verlinde, C. L.; Opperdoes, F. R.; Hol, W. G.; Gelb, M. H. **Structure-based design of submicromolar, biologically active inhibitors of trypanosomatid glyceraldehyde-3-phosphate dehydrogenas.** (1999). *Proc. Natl. Acad. Sci. USA.* **96**, 4273-8.
- [18] Fred R. Opperdoes & Paul A.M. Michels, **Enzymes of carbohydrate metabolism as potential drug targets,** (2001). *International journal for parasitology* , volume 31, p.482-490.
- [19] K.Montin, C.Cervellati, F.Dalocchio & S.Hanau, **Thermodynamic characterization of substrate and inhibitor binding to *Trypanosoma brucei* 6-phosphogluconate dehydrogenase.** (2007) *the Febs journal.* **274**, p. 6426-6435.
- [20] Gupta S, Igoillo-Esteve M, A.M.Michels P and Cordeiro A, **Glucose-6-phosphate dehydrogenase of trypanosomatids: characterization, target validation, and drug discovery.** (2011) *Molecular Biology International*, volume 2011 , Article ID 135701.
- [21] Hanau S, Rinaldi E, Dalocchio F, Gilbert IH, Dardonville C, Adams MJ, Gover S, Barrett MP. **6-phosphogluconate dehydrogenase: a target for drugs in African trypanosomes.** (2004). *Curr Med Chem.* **11**(19):2639-50.
- [22] C. Phillips, J. Dohnalek, S. Gover, M.P. Barrett, M.J. Adams, **A 2.8 Å resolution structure of 6-phosphogluconate dehydrogenase from the protozoan parasite *Trypanosoma brucei*: comparison with the sheep enzyme accounts for differences in activity with coenzyme and substrate analogues.** (1998) *J. Mol. Biol.* **282.** 667–681].
- [23] Barrett, M.P., Gilbert, I.H. **Perspectives for new drugs against Trypanosomiasis and Leishmaniasis.** (2002) *Curr. Top. Med. Chem,* **11**, 3205-3214.



- [24] Dardonville, C., Rinaldi, E., Barrett, M.P., Brun, R., Gilbert, I.H., Hanau, S. **Selective Inhibition of *Trypanosoma brucei* 6-Phosphogluconate Dehydrogenase by High-Energy Intermediate and Transition-State Analogues.** (2004) *J. Med. Chem.* 47, 3427-3437.
- [25] Ruda GF, Alibu VP, Mitsos C, Bidet O, Kraiser M, Brun R, Barrett MP & Gilbert IH **Synthesis and biological evaluation of phosphate prodrugs of 4- phospho-D-erythronohydroxamic acid, an inhibitor of 6- phosphogluconate dehydrogenase.** (2007) *ChemMedChem* , 2, 1169-1180.
- [26] Pasti, C., Rinaldi, E., Cervellati, C., Dallochio, F., Hardre, R., Salmon, L., Hanau S. **Sugar Derivatives as New 6-Phosphogluconate Dehydrogenase Inhibitors Selective for the Parasite *Trypanosoma brucei*.** ( 2003) *Bioorg. Med. Chem.* 11, 1207-1214.
- [27] Adams MJ, Ellis GH, Gover S, Naylor CE & Phillips C **Crystallographic study of coenzyme, coenzyme analogue and substrate binding in 6 phosphogluconate dehydrogenase: implications for NADP specificity and the enzyme mechanism.** (1994). *Structure*, 2, 651–668.
- [28] Karsten WE, Chooback L & Cook PF **Glutamate 190 is a general acid catalyst in the 6-phosphogluconate dehydrogenase-catalyzed reaction.** (1998). *Biochemistry.* 37, 15691–15697
- [29] Rippa M, Bellini T, Signorini M & Dallochio F **The stabilization by a coenzyme analog of a conformational change induced by substrate in the 6-phosphogluconate dehydrogenase.** (1979) *Arch Biochem Biophys* , 196, 619–623
- [30] Rippa M, Giovannini PP, Barrett MP, Dallochio F & Hanau S, **6 Phosphogluconate dehydrogenase: the mechanism of action investigated by a comparison of the enzyme from different species.** (1998). *Biochim Biophys Acta*,1429, 83–92.
- [31] Rippa M, Hanau S, Cervellati C, Dallochio F. **6Phosphogluconate dehydrogenase: Structural symmetry and functional asymmetry.** (2000). *Protein and Peptide Letters*, Vol 7. N5 p.p 341-348
- [32] Topham CM, Matthews B & Dalziel K **Kinetic studies of 6- phosphogluconate dehydrogenase from sheep liver.** (1986) *Eur. J. Biochem.*, 156, 555–567.
- [33] Rippa M., Signorini M. e Pontremoli S. **Purification and properties of two forms of 6-phosphogluconate dehydrogenase from *Candida utilis*.** (1967). *Eur. J. Biochem.*, 1, 170-178
- [34] Rippa M., Signorini M. e Pontremoli S. **Evidences for the involvement of achistidine residue in the binding of the substrate to the 6-phosphogluconate dehydrogenase.,** (1972) *Arch. Biochem. Biophys.* 150, 503-510.

- [35] Dallochio, F., Signorini M. Rippa M., **Evidence for the proximity of a cysteinyl and a tyrosyl residue in the active site of 6-phosphogluconate dehydrogenase.** (1978). Arch. Biochem. Biophys. 185, 57-60.
- [36] Hanau, S., Dallochio, F. and Rippa, M. **Use of trinitrobenzenesulfonate for affinity labeling of lysine residues at phosphate binding sites of some enzymes.** (1993). Arch. Biochem. Biophys. 302, 218-221.
- [37] Hanau, S., Dallochio, F. and Rippa M, **Subunits asymmetry in the ternary complex of lamb liver 6-phosphogluconate dehydrogenase detected by a NADP analogue.** (1992). Biochem. Biophys. Acta. 1159, 262-266.
- [38] Hanau S, Dallochio F & Rippa M, **Is there an alternating site cooperativity between the two subunits of lamb liver 6-phosphogluconate dehydrogenase?** (1993). Biochem J. 291, 325-326.
- [39] Adams MJ, Ellis GH, Gover S, Naylor CE & Phillips C **Crystallographic study of coenzyme, coenzyme analogue and substrate binding in 6- phosphogluconate dehydrogenase: implications for NADP specificity and the enzyme mechanism.** (1994). Structure. 2, 651-668.
- [40] Hannaert, V., Saavedra, E., Duffieux, F., Szikora, J.P., Rigden, D.J., Michels, P.A.M., Opperdoes, F.R. **Plant-like traits associated with metabolism of Trypanosoma parasites.** (2003). Proc. Natl. Acad. Sci. USA. 100, 1067-1071.
- [41] Hanau, S., Rinaldi, E., Dallochio, F., Gilbert, I. H., Dardonville, C., Adams, M.J., Gover, S., Barrett, M.P. **6-phosphogluconate dehydrogenase: a target for chemotherapy in African trypanosomiasis.** (2004). Curr. Med. Chem. 11, 1345-1359.
- [42] Krepinsky, K., Plaumann, M., Martin, W., Schnarrenberger, C. **Purification and cloning of chloroplast 6-phosphogluconate dehydrogenase from spinach.** (2001). Eur. J. Biochem. 268, 2678-2686.
- [43] Barrett, M. P., Le Page, R.W.F. **A 6-phosphogluconate dehydrogenase gene from Trypanosoma brucei.** (1993). Mol. Biochem. Parasitol. 57, 89-100.
- [44] Corpet F., **Multiple sequence alignment with hierarchical clustering,** (1988). Nucleic Acids Res. 16(22). 10881-90.
- [45] Gouet P., Robert X., Courcelle E., **ESPrpt/ENDscript : Extracting and rendering sequence and 3D information from atomic structures of proteins.** (2003). Nucleic Acids Res., 31(13) :3320-3323.
- [46] Emmanuel Tetaud, Stefania Hanau, Jeremy M. Wells, Richard W.F. Le Page, Margaret J. Adams, Scott Arkison & Michael P. Barret, **6-phosphogluconate dehydrogenase from Lactococcus lactis: a role for arginine residues in binding substrate and coenzyme,** (1999). Biochem. J. 338, 55-60.

- [47] Philips, C.; Gover. S.; Adams, M. J. **Structure of 6-phosphogluconate dehydrogenase refined at 2 Å resolution.** (1995). *Acta Crystallogr. D Biol. Crystallogr.* 51;290-304.
- [48] Sundaramoorthy R.; Iulek J.; Barrett M.P.; Bidet O.; Ruda G. F.; Gilbert I.H.; Hunter W.N.; **Crystal structures of a bacterial 6-phosphogluconate dehydrogenase reveal aspects of specificity, mechanism and mode of inhibition by analogues of high-energy reaction intermediates.** (2007). *FEBS J.* 274(1) : 275-286.
- [49] Dyson, J. E. D.; d’Orazio, R. E.; and Hanson, W. H. **Sheep liver 6-phosphogluconate dehydrogenase: isolation procedure and effect of pH, ionic strength, and metal ions on the kinetic parameters.** (1973). *Arch. Biochem & Biophys.* 154:623-35.
- [50] Chen YY, Ko TP, Chen WH, Lo LP, Lin CH, Wang AH. **Conformational changes associated with cofactor/substrate binding of 6-phosphogluconate dehydrogenase from Escherichia coli and Klebsiella pneumoniae: Implications for enzyme mechanism.** (2010). *J Struct Biol.*;169(1):25-35.
- [51] Emmanuel Tetaud , Stefania Hanau., Jeremy M. Wells., Richard W. F. Le Page., Margaret J. Adams, Scott Arkison. and Michael P. Barrett. **6-Phosphogluconate dehydrogenase from Lactococcus lactis : a role for arginine residues in binding substrate and coenzyme.** (1999). *Biochem. J.* 338, 55±60
- [52] Gualdron-López M, Vapola MH, Miinalainen IJ, Hiltunen JK, Michels PA, Antonenkov VD. **Channel-forming activities in the glycosomal fraction from the bloodstream form of Trypanosoma brucei** (2012). *PLoS One.* 7(4): e34530.
- [53] Hanau, S, K. Montin, I.H. Gilbert, M.P. Barret and F. Dallochio. **Inhibitors of Trypanosoma brucei 6- Phosphogluconate Dehydrogenase.** (2007). *Current Bioactive Compounds*, 3, 161-169
- [54] Randy O. **African Trypanosomiasis (Sleeping Sickness)** (2012)
- [55] WHO. **Trypanosomiasis, Human African (sleeping sickness).** (2012). Fact sheet N°259
- [56] Rendina, A. R., Hermes, J. D., and Cleland, W. W. **Biochemistry.** (1984) 23,6257–6262.
- [57] Hwang, C. C., Berdis, A. J., Karsten, W. E., Cleland, W. W., and Cook, P. F. **Biochemistry** 37. (1998). 12596–12602
- [58] Hwang, C. C., and Cook, P. F. **Biochemistry** 37. (1998) 15698–15702].

- [59] Riddles P.W., Blakeley R.L., Zerner B. **Reassessment of Ellman's reagent in Methods in Enzymology.** (1983) 91, 49-60. Hirs c.H.W. & Timasheff S.N. eds., Academic Press.
- [60] Laemmli, U. K. **Cleavage of structural proteins during the assembly of the head of bacteriophage T4.** (1970). *Nature* 227, 680-685.
- [61] Vasiliki E. Fadouloglou; Michael Kokkinidis Nicholas M. Glykos; **Determination of protein oligomerization state: Two approaches based on glutaraldehyde crosslinking.** (2008). *Analytical Biochemistry* . 373, Issue 2 404–406
- [62] [http://www.malvern.com/LabEng/technology/dynamic\\_light\\_scattering/dynamic\\_light\\_scattering.htm?gclid=CKqypYmqrrUCFcNV3goddnsAyg](http://www.malvern.com/LabEng/technology/dynamic_light_scattering/dynamic_light_scattering.htm?gclid=CKqypYmqrrUCFcNV3goddnsAyg)
- [63] Isabelle Migneault, Catherine Dartiguenave, Michel J. Bertrand, and Karen C. Waldron. **Glutaraldehyde: behavior in aqueous solution, reaction with proteins, and application to enzyme crosslinking.** (2004). *BioTechniques*. 37:790-802.
- [64] T.J.A. Johnson; **Glutaraldehyde Cross-Linking, Fast and Slow Modes.** (1993). *Biocatalyst Design for Stability and Specificity* (1993) , 283-294.
- [65] Ulf N, Malcolm C, Brendan F, Paul V, Chris G, Sandrine M, Juntao C., Liang Z, Yanglinglu3, Fei S3, Junming, Stephen E, Harding M. **Dynamic light scattering as a relative tool for assessing the molecular integrity and stability of monoclonal antibodies** (2007) .*Biotechnology and Genetic Engineering Reviews* - Vol. 24, 117-128.
- [66] [http://www.malvern.com/LabEng/technology/dynamic\\_light\\_scattering/dynamic\\_light\\_scattering.htm?gclid=CKqypYmqrrUCFcNV3goddnsAyg](http://www.malvern.com/LabEng/technology/dynamic_light_scattering/dynamic_light_scattering.htm?gclid=CKqypYmqrrUCFcNV3goddnsAyg)
- [67] B.J. Berne, R. Pecora; **Dynamic Light Scattering with Applications to Chemistr.** (2000).*Biology and Physics General Publishing Company, Ltd, Toronto, Canada.*
- [68] A. Ortega, D. Amoros, J. Garcia de la Torre, **Prediction of hydrodynamic and other solution properties of rigid proteins from atomic- and residue-level models.** (2011). *Biophys. J.* 101 892-898.
- [69] Raschke S, Guan J, Iliakis G. **Application of alkaline sucrose gradient centrifugation in the analysis of DNA replication after DNA damage.** (2009). *Methods Mol Biol.* 521:329-42.
- [70] Duff, Jr., M. R., Grubbs, J., Howell, E. E. **Isothermal Titration Calorimetry for Measuring Macromolecule-Ligand Affinity.** (2011). *J. Vis. Exp.* (55), e2796, doi:10.3791/2796
- [71] K.P. Murphy, B.M. Baker, P. Edgcomb, J.R. Horn. **Structural energetics of serine protease inhibition,** (1999). *Pure Appl. Chem.*, 71, 1207-1213

- [72] H Fukada, k Takahashi, **Enthalpy and heat capacity changes for the proton dissociation of various buffers components in 0,1 M potassium chloride.** (1998). *Proteins* 33. 159-166.
- [73] I. Dominguez-Perez, R. Tellez-Sanz, I. Leal, L.M. Ruiz-Perez, D. Gonzalez-Pacanowska, L. Garcia-Fuentes, **Calorimetric determination of thermodynamic parameters of 2V-dUMP binding to Leishmania major dUTPase.** (2004). *Biochim. Biophys. Acta* 1702. 33-40.
- [74] S. Hanau, K. Montin, C. Cervellati, M. Magnani and F. Dallochio. **“6-Phosphogluconate dehydrogenase mechanism: evidence for allosteric modulation by substrate”** (2010). *The Journal of Biological Chemistry* 285: 21366-21371.
- [75] F. Dallochio, M. Matteuzzi, T. Bellini, **Effect of the substrate on the binding of coenzyme and coenzyme analogues to 6-phosphogluconate dehydrogenase from *Candida utilis*,** (1981). *J. Biol. Chem.* 256. 10778-10780.
- [76] N.E. Price, P.F. Cook, **Kinetic and chemical mechanisms of the sheep liver 6-phosphogluconate dehydrogenase.** (1996). *Arch. Biochem. Biophys.* 336. 215-223.
- [77] M. Rippa, M. Signorini, F. Dallochio, **Differentiation between the structural and redox roles of TPNH in 6-phosphogluconate dehydrogenase.** (1972). *Biochem. Biophys. Res. Comm.* 48. 764-768.
- [78] M. Rippa, M. Signorini, F. Dallochio, **A role for the pyridine nitrore of reduced triphosphopyridinenucleotide in an enzymatic catalysis.** (1973). *FEBS Lett.* 36. 148-150.
- [79] S. Hanau, F. Dallochio and M. Rippa, **NADPH activates a decarboxylation reaction catalysed by lamb liver 6-phosphogluconate dehydrogenase.** (1992). *Biochim. Biophys. Acta* 1122 273-277.
- [80] C.N. Cronin, D.P. Nolan, H.P. Voorheis, **The enzymes of the classical pentose phosphate pathway display differential activities in procyclic and bloodstream forms of *Trypanosoma brucei*.** (1989). *FEBS Lett.* 244. 26-30.
- [81] C.J. Lin, H.Y. Ho, M.L. Cheng, T. H. You, J.S. Yu, D.T. Chiu, **Impaired dephosphorylation renders G6PD-knockdown HepG2 cells more susceptible to H<sub>2</sub>O<sub>2</sub>-induced apoptosis.** (2010). *Free Rad. Biol. Med.* 49. 361-373
- [82] V.P. Sukhatme, B. Chan, **Glycolytic cancer cells lacking 6-phosphogluconate dehydrogenase metabolize glucose to induce senescence.** (2012). *FEBS Lett.* 586. 2389-2395.
- [83] Chirgwin J. M. & Noltmann E. A., **The enediolate analogue 5-phosphoarabinonate as a mechanistic probe for phosphoglucose isomerase,** *The Journal of Biological Chemistry*, 1975, vol. 250, pp. 7272-7276.),

- [84] S.J. Hubbard, J.M. Thornton, **NACCESS, Computer Program.** (1993. )Department of Biochemistry and Molecular Biology, University College London, London, UK.
- [85] Hanau S., Rippa M., Dallochio F. & Barrett M.P., **6-phosphogluconate dehydrogenase from *Trypanosoma brucei*: kinetic analysis and inhibition by trypanocidal drugs**, European Journal of Biochemistry, 1996, vol. 240, pp. 592-599).
- [86] Carlo Cervellati, Franco Dallochio, Carlo M. Bergamini and Paul F. Cook. **Role of Methionine-13 in the Catalytic Mechanism of 6-Phosphogluconate Dehydrogenase from Sheep Liver.** (2005). *Biochemistry.* **44**, 2432-2440